A Review of Nonlinear Static Analyses of Planar Steel Frames

FINAL YEAR PROJECT UG 2016

By:

Asghar Arshad Jadoon	**177257 (Group leader)**
M. Sarib Shahid	**176985**
Malik Arsalan	**174571**
Talha Maqbool	**185270**

NUST Institute of Civil Engineering

School of Civil and Environmental Engineering

National University of Science and Technology, Islamabad, Pakistan

2020

This is to certify that the

Report entitled

A Review of Nonlinear Static Analyses of Planar Steel Frames

Submitted by

Asghar Arshad Jadoon   **177257 (Group leader)**

M. Sarib Shahid   **176985**

Malik Arsalan   **174571**

Talha Maqbool   **185270**

Has been accepted towards the requirements for the undergraduate degree **Bachelors of Engineering in Civil Engineering**

_____

Lec. Samiullah Khan Bangash,

NUST Institute of Civil Engineering (NICE),

School of Civil and Environmental Engineering (SCEE),

National University of Sciences and Technology, Islamabad, Pakistan.

Acknowledgements

Thanks be to Allah Almighty, the most Merciful and the most Beneficial.

We are indebted to our project supervisor Lec Samiullah Bangash who helped us throughout the project and provided assistance every step of the way. His sheer determination motivated us to carry out our task in an effective and practical manner. His profound understanding of nonlinear analysis and computational mechanics is what enabled us to execute this project in an adequate manner. It could not have been possible without him.

We would also like to pay special regards to the staff of Structure Lab, especially Mr. Matiullah Shah (Lab Engineer), for helping us out throughout the project.

We wish to express our deepest gratitude to everyone who was directly or indirectly a part of this project and played an essential role in its completion.

Table of Contents

LIST OF FIGURES

1. Abstract

For several years, alignment charts and moment amplification factors were the basis for design of columns and beams subjected to combined loadings. However, in recent years, research has been devoted to developing a rigorous second order analysis computational framework. While many commercial software now provide embedded second order facility, many designers still lack the theoretical and more importantly, the algorithmic know how of the machinery behind these software. Our research goal is to unravel this machinery right down to its algorithmic detail so that a structural analyst can understand the assumptions, limitations and nuances of nonlinear analysis. The objective of this study is threefold: First, to give a detailed insight into the nonlinear analyses, while creating a MATLAB learning suite, to help with the understanding of the subject. We will use MASTAN2 for the verification of our codes. Second, to equip the future researchers with the preliminary knowledge required in the more active areas of research. And third, to aid the engineers working in the field by familiarizing them with the rigorous second order analysis for a more accurate stability design. MATLAB codes were developed and verified for the critical load analyses and the load deflection analyses while providing a detailed explanation of the algorithmic procedures involved along with the flowcharts. This study will serve to develop a sound understanding of the basics of steel stability for the new researchers and will help in acquainting the design engineers with rigorous second order analysis.

2. Literature Review

In literature review, we start off with a detailed investigation of Euler's perfect column and the assumptions that it makes. We then study the effects of these assumptions in the form of residual stresses, initial imperfections and the effective length factor. We then move towards alignment charts for the calculation of the effective length factor for elastic end restraints. We also introduce the nonlinearity in systems and study their sources and give an overview of the matrix approach.

2.1 Column Buckling

This section discusses the case of columns in which they are subjected to axial loading. These columns are continuous and hence their solution is not algebraic, rather it is differential.

2.1.1 Euler's Column

In 1757, a Swiss mathematician Leonhard Euler came up with an equation for finding the critical load for a column at which the column buckles. However, in order to get to this equation, Euler made some assumptions. He assumed the column to be perfectly straight, prismatic and elastic. We will study the implications of these assumptions in the following sections. For now, we will derive Euler's equation for column buckling.

Consider a prismatic column having length **L** and moment of inertia **I**, under an axial load **P** shown in **Figure 01** below.
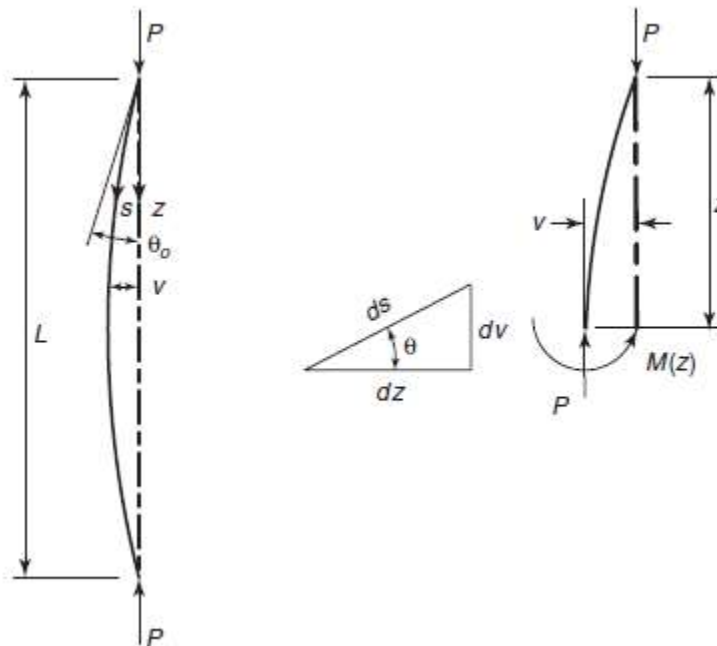
Figure 1 Buckled shape of elastic column

According to Euler, the column remains perfectly straight until bifurcation takes place and it buckles. At the point of bifurcation, an infinitesimally close deflected shape is formed which is shown in figure 1. Euler made use of this deflected shape to formulate equilibrium and derive the critical load formula. The deflection is given by v and the end slope at which column deforms is θ_o.

The external bending moment is equal to the applied axial force multiplied with the deflection.

$$M(z) = Pv \qquad\qquad \text{--2.1}$$

In order to maintain equilibrium, this applied moment has to be equal to the internal moment, i.e.

$$Pv = -EI\emptyset \qquad\qquad \text{--2.2}$$

Where $\emptyset$ is the curvature and can be denoted as

$$\emptyset = \frac{d\theta}{ds} \qquad\qquad \text{--2.3}$$

Rearranging equation 2.2, dividing by EI, and inserting $\emptyset$ from equation 2.3, we get

$$\frac{P}{EI}v + \frac{d\theta}{ds} = 0 \qquad\qquad \text{--2.4}$$

Differentiating once, we get

$$\frac{P}{EI}\frac{dv}{ds} + \frac{d^2\theta}{ds^2} = 0 \qquad\qquad \text{--2.5}$$

Substituting $\frac{dv}{ds} = \sin\theta$ and $\frac{P}{EI} = k^2$, we get

$$\frac{d^2\theta}{ds^2} + k^2 \sin\theta = 0 \qquad\qquad \text{--2.6}$$

Equation 2.6 is the exact differential equation proposed by Euler. Now, consider figure 2 given below.
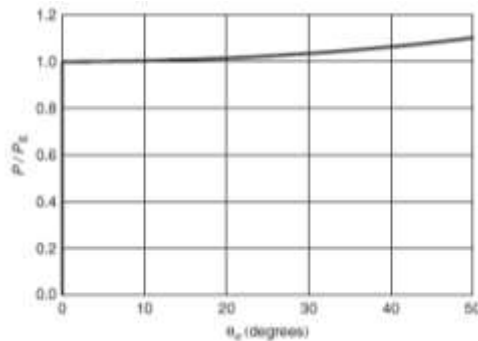
Figure 2 Post-buckling end rotation of a pinned-end column

It can be seen that hardening begins only at large θ i.e. $\theta \sim 20°$, so we can safely assume small deflections for which

$$sin\theta = \theta \qquad \text{--2.7}$$

By doing so, we can simplify the differential equation of equation 2.6 by the process of linearization and it becomes

$$\frac{d^2\theta}{ds^2} + k^2\theta = 0 \qquad \text{--2.8}$$

Which can be written as

$$\theta'' + k^2\theta = 0 \qquad \text{--2.9}$$

Similarly, we can prove that

$$v'' + k^2v = 0 \qquad \text{--2.10}$$

The general solution for 2.10 is given as

$$v = A \sin kz + B \cos kz \qquad \text{--2.11}$$

As our column is pinned at both ends, we know that there can be no deflections at the ends. This gives us our two boundary conditions.

$$v(0) = 0 \qquad \text{--2.12}$$
$$v(L) = 0 \qquad \text{--2.13}$$

Now that we have two unknowns and two boundary conditions, we can solve equation 2.11 which gives us

$$A \sin kL = 0 \qquad \text{--2.14}$$

Since assuming A=0 gives us a trivial solution, we know that

$$sinkL = 0 \qquad \text{--2.15}$$

Assuming $kL = 0$ will satisfy equation 2.15, but that will again be of no use to us. So, for now we assume the first possible solution that satisfies 2.15 and is not trivial, i.e.

$$kL = \pi \qquad \text{--2.16}$$

Substituting equation 2.16 in $k^2 = \frac{P}{EI}$, we obtain the classic Euler buckling equation:

$$P_E = \frac{\pi^2 EI}{L^2} \qquad \text{--2.17}$$

2.1.2 Initial Imperfections

While deriving the column buckling equation, Euler assumed the column to be perfectly straight and free of any initial imperfections. This implied that there was no bending in the column prior to buckling. However, there can exist initial imperfections in the column in the form of:

- Initial Crookedness
- Load Eccentricity
- Lateral Loading

(a) Initial crookedness, v_o (b) Load eccentricity, e (c) Lateral load, q
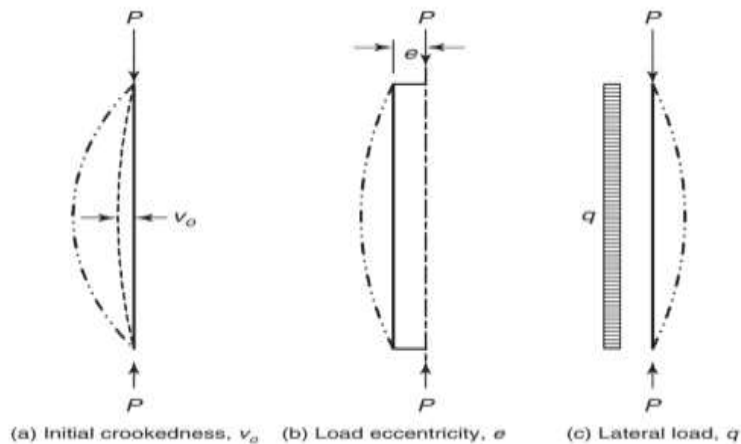
Figure 3 Initial imperfections

The presence of these initial imperfections nullify the assumption that the column remains perfectly straight before it buckles. These imperfections impart an additional moment in the column in the form of $P\delta$ effect which will be discussed later. We can derive the magnification factors for all these cases (Ref. 1). Figure 4 shows a plot of the ratio of applied load to the buckling load against the magnification factors for these defects.
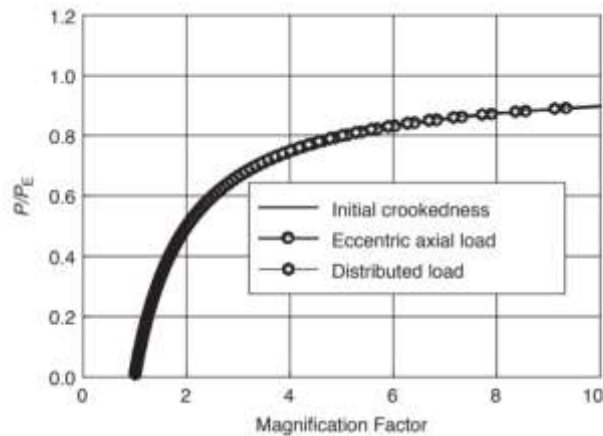
Figure 4 Comparison of magnification factors

It can be seen from figure 4 that the magnification factor curves for all the cases are essentially on top of each other. This allows us to use a single, representative equation that matches the response, which is

$$MF = \frac{1}{1 - P/P_E} \qquad \qquad \text{--2.18}$$

Equation 2.18 is analogous to the B1 amplifier used in AISC 360 for the amplifier based procedures and accounts for the additional moment that arises due to the member sway known as the Pδ effect.

2.1.3 Residual Stresses

Euler assumes the column to behave in a perfectly elastic manner. However, that is not the case normally due to the presence of residual stresses which are an inevitable part of the manufacturing process of hot-rolled steel. Due to non-uniform cooling of members or by straightening of flange members in wide flange shapes, flange tips tend to cool faster than the junctions. Similarly, central part of web tends to cool faster than the junctions. As a result, the tensile stresses develop at junction and compressive stresses at tips as shown in figure 5.
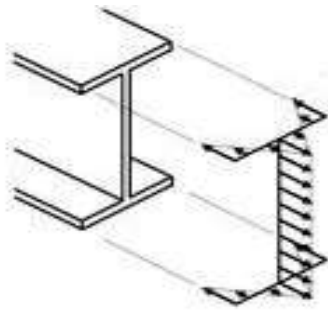
Figure 5 Usual residual stress profile for W-shapes

Due to the presence of these residual stresses, the material experiences partial yielding and is no longer elastic. Residual stresses decrease the strength of material and causes the member to start yielding before its yield point is reached.

2.1.3.1 Numerical Example
Consider the W-shape in in figure 6 and its residual stress profile.

Given Data
Flange Plate: PL 12" x 0.75"
Web Plate: PL 12" x 0.5"
ASTM Gr42
F_y= 42 ksi
F_r= 10 ksi
E=29000 ksi

6
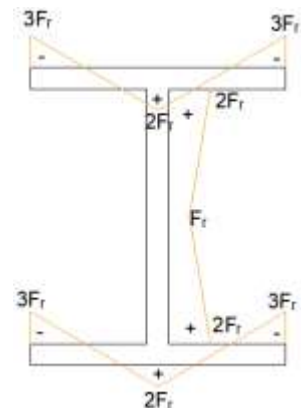
Our goal is to make stress-strain equations and we do this by analyzing the residual stress profiles of both the flange and the web. Note that the highest compressive residual stress is present at the flange tips i.e. -30 ksi. This implies that we need to apply -12 ksi stress for it to reach the yield stress. This will be the stage 1 and as it is evident, it will be linear as there is no yielding taking place.

$$\Delta F_1 = -12 \; ksi$$

$$E = 29000 \; ksi$$

$$\Delta \varepsilon_1 = \frac{\Delta F_1}{E} = -0.0004138$$

Now the highest compressive stress is present at the center of the web i.e. -2 ksi. In order to get it to the yield surface, we need to apply a compressive stress of 40 ksi. However, this time we cannot assume the response to be linear as there will be partial yielding. We are going to assume a second order curve for the stress as:

$$\sigma_2 = A\varepsilon^2 + B\varepsilon + C$$

The reason why we know this is true is because of the fact that in general, if the residual stress profile is of the order n, $\sigma(\varepsilon)$ is of the order n+1. Also,

$$E_2(\varepsilon_2) = \frac{d\sigma_2}{d\varepsilon_2} = 2A\varepsilon + B$$

Now, proceeding with the second stage, we have three unknowns in the form of A, B and C. In order to solve this equation, we need to have three boundary conditions.

$$2A(-0.0004138) + B = 29000 \qquad \textbf{BC1}$$

$$\sigma_2(-0.0004138) = -12ksi \qquad \textbf{BC2}$$

$$\Delta\varepsilon_2 = \frac{\Delta f_2}{E} = \frac{-40}{29000} = -0.001379$$

$$\varepsilon_2 = \varepsilon_1 + \Delta\varepsilon_2$$

$$\Delta\varepsilon_2 = -0.004138 - 0.001379$$

$$\Delta\varepsilon_2 = -0.001793$$

$$\sigma_2(-0.001793) = -40ksi \qquad \textbf{BC3}$$

Now that we have formulated three boundary conditions, we can find the values of the unknowns which come out to be

A=6306827.05
B=-34219.5301
C=1.08012

Now in order to reach full yielding, we need to apply stress of -10 ksi and using similar procedure as above, we can formulate boundary conditions and find the unknowns. Shown below are the stress-strain equations for all the three stages of stress application.

<u>Range 1:</u> $\sigma_1 = E\varepsilon_1$

<u>Range 2:</u> $\sigma_2 = 6306827.052\varepsilon_2{}^2 - 34219.5301\varepsilon_2 + 1.08012$

<u>Range 3:</u> $\sigma_3 = 16898171.62\varepsilon_3^2 - 72222.7855\varepsilon_3 + 35.1712$

This implies that before yielding begins, i.e. in range 1, we use our initial modulus of elasticity. But once yielding has started, we switch to using the tangent modulus due to the partial yielding that takes place in range 2 and 3.

$$F_{CR} = \frac{\pi^2 E_t}{(\frac{KL}{r})^2} \qquad F_{CR} > F_P$$

$$F_{CR} = \frac{\pi^2 E}{(\frac{KL}{r})^2} \qquad F_{CR} \leq F_P$$
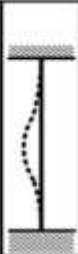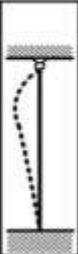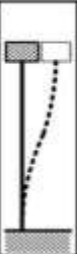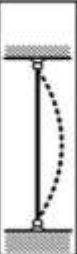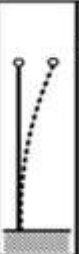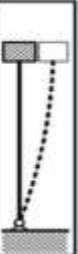
where $F_P = 12ksi$

2.1.4 Effective Length Factor

Euler assumed the column to be pinned at both ends but for different boundary conditions, Euler's formula takes the following form

$$P_E = \frac{\pi^2 EI}{(KL)^2} \qquad\qquad \text{--2.19}$$

Where K is the effective length factor which varies with the boundary conditions. It is fairly simple to calculate the effective length factor for fundamental boundary conditions that are shown in figure 6. However, we do not normally encounter these fundamental boundary conditions and are normally faced with elastic end restraints. In order to find the effective length factor for these elastic restraints, alignment charts were developed which will be discussed in detail in the following section.

Buckled shape of column shown by dashed line						
Theoretical K value	0.5	0.7	1.0	1.0	2.0	2.0
Recommended design value K	0.65	0.80	1.2	1.0	2.10	2.0

Figure 6 Effective length factor for fundamental boundary conditions

2.2 Alignment Charts

In this section, we will start by looking at the stability of a frame rather than isolated columns. In the case of frames, we encounter elastic end restraints which, as discussed before, make it difficult to calculate the effective length factor. We will then proceed to the derivation of alignment charts for both the sway permitted and sway prohibited cases. We will also discuss some assumptions that are made in the process of developing these alignment charts. Alignment charts serve as a tool for easily finding the effective length for elastic end restraints. The effective length method for stability in AISC 360 is based on these alignment charts.

2.2.1 Stability of a Frame

Consider the frame shown in figure 7. The column has a pin joint at the base and is restrained by the beam at the top. Column has the length L_c is subjected to the load **P.**
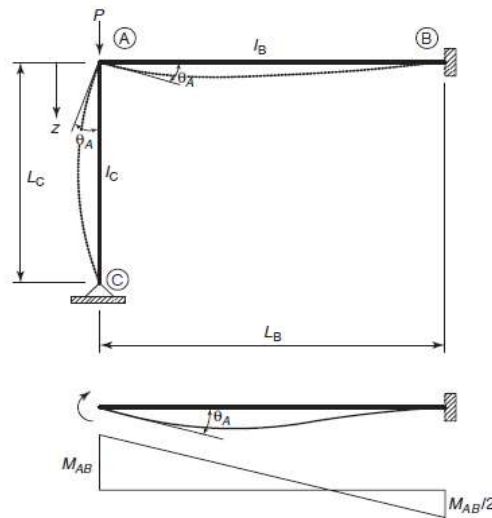
Figure 7 Elastically restrained assembly

As the column is pinned at the base, the boundary conditions at the bottom are:

$$v(L) = v''(L) = 0$$

In order to formulate boundary conditions at the top, we know that there is no deflection there. Also, the moment in the column must be equal to the moment in the beam in order for them to cancel each other out. Solving for the moment in the beam at the joint gives us:

$$M_{AB} = \frac{4EI_B}{L_B} \theta_A = \alpha \theta_A = \alpha v'(0)$$

Here α is the spring constant which is equal to $\frac{4EI_B}{L_B}$ when the far end of the beam is fixed. Top end of the column has the moment:

$$M_{AC} = -EI_C v''(0)$$

Equating both moments gives us the fourth boundary condition. So now we have four boundary conditions as shown.

$$v(L_C) = 0$$
$$v''(L_C) = 0$$
$$v(0) = 0$$
$$\alpha v'(0) - EI_C v''(0) = 0$$

The homogeneous solution is $v = A + Bz + C\sin kz + D\cos kz$. Solving this equation with the help of boundary conditions gives us the following determinant:

$$\begin{vmatrix} 1 & 0 & 0 & 1 \\ 0 & \alpha & \alpha k & P \\ 1 & L & \sin kL_C & \cos kL_C \\ 0 & 0 & -k^2\sin kL_C & -k^2\cos kL_C \end{vmatrix} = 0$$

Evaluating the determinant gives us the following Eigen function:

$$\tan kL_c = \frac{\alpha kL_C}{PL_C + \alpha} = \frac{\gamma kL_C}{(kL_C)^2 + \gamma}$$

Where

$$\gamma = \frac{\alpha L_C}{EI_C} \qquad\qquad \text{--2.20}$$

Equation 2.20 is the buckling equation for a column with a spring at one end and a pin joint at another.

2.2.2 Non-Sway Case

In this section, we will discuss the case in which a column is restrained by springs at both ends. The two ends of the column do not move with respect to each other, i.e. the column is not allowed to sway. Consider the column shown in figure 8.
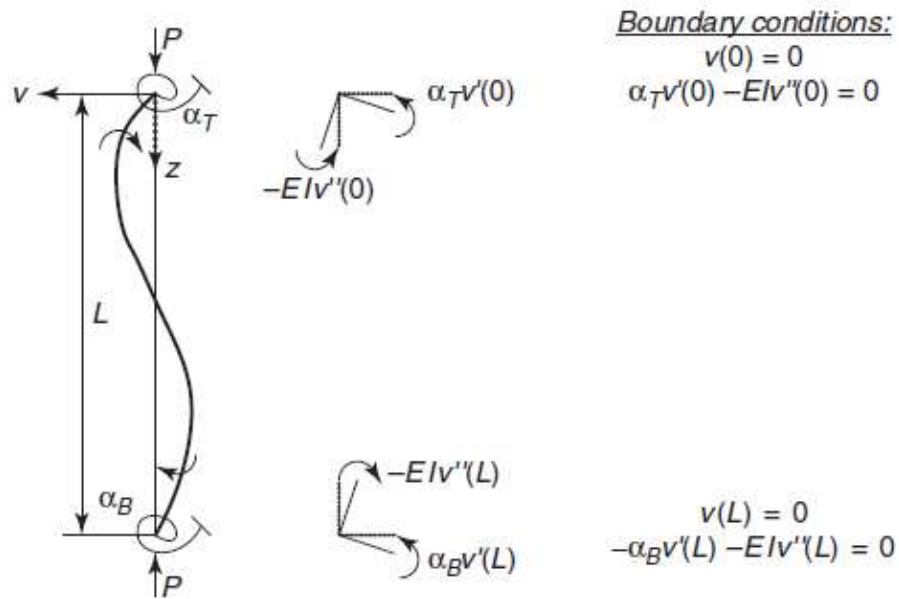
Figure 8 Non-sway restrained column

Using the boundary conditions to solve the homogeneous equation, we can formulate the determinant as:

$$\begin{vmatrix} 1 & 0 & 0 & 1 \\ 1 & L & \sin kL & \cos kL \\ 0 & \alpha_T & \alpha_T k & EIk^2 \\ 0 & -\alpha_B & -\alpha_B k \cos kL + EIk^2 \sin kL & \alpha_B k \sin kL + EIk^2 \cos kL \end{vmatrix} = 0$$

We will introduce the following non-dimensional spring constants to simplify the determinant:

$$R_T = \frac{\alpha_T L}{EI} \qquad R_B = \frac{\alpha_B L}{EI}$$

Evaluating the determinant after substituting R_T and R_B, we get the following equation:

$$-2R_T R_B + \sin kL[R_T R_B kL - kL(R_T + R_B) - (kL)^3] + \cos kL[2R_T R_B + (kL)^2(R_T + R_B)] = 0 \quad \text{--2.21}$$

Assuming the beams to be pinned at ends as shown in figure 9, we can evaluate the two spring constants α_T and α_B as:

$$\alpha_T = \frac{2EI_{gT}}{L_{gT}} \rightarrow R_T = \frac{2\left(\frac{I_{gT}}{L_{gT}}\right)}{\frac{I_C}{L_C}} \qquad\qquad \alpha_B = \frac{2EI_{gB}}{L_{gB}} \rightarrow R_B = \frac{2\left(\frac{I_{gB}}{L_{gB}}\right)}{\frac{I_C}{L_C}}$$
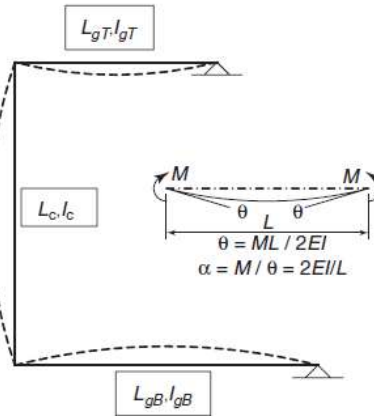
Figure 9 Non-sway sub-assembly

Manipulating equation 2.21 results in the following equation:

$$\frac{(kL)^2 G_T G_B}{4} - 1 + \frac{G_T + G_B}{2}\left(1 - \frac{kL}{\tan kL}\right) + \frac{2\tan\frac{kL}{2}}{kL} = 0 \qquad\qquad \text{--2.22}$$

Where

$$G_T = \frac{\frac{I_C}{L_C}}{\frac{I_{gT}}{L_{gT}}} \qquad\qquad G_B = \frac{\frac{I_C}{L_C}}{\frac{I_{gB}}{L_{gB}}}$$

Solving equation 2.22 for the smallest value of kL that satisfies the equation results in the critical buckling load.

$$\frac{(\frac{\pi}{k})^2 G_T G_B}{4} - 1 + \frac{G_T + G_B}{2}\left(1 - \frac{\frac{\pi}{k}}{\tan\frac{\pi}{k}}\right) + \frac{2\tan\frac{\pi}{2k}}{\frac{\pi}{k}} = 0 \qquad\qquad \text{--2.23}$$

Equation 2.23 serves as the basis for the alignment chart for the non-sway case in AISC 360.

2.2.3 Sway Permitted Case

Consider the column in figure 10 which is restrained by rotational and translational springs at both ends.

Figure 10 Column with rotational and translational springs
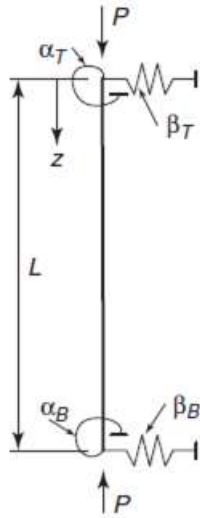
$$@\,z = 0:\quad -EIv''' - Pv' = \beta_T v$$
$$-EIv'' = -\alpha_T v'$$
$$@z = L:\quad -EIv''' - Pv' = -\beta_B v$$
$$-EIv'' = \alpha_B v'$$

We will introduce the following variables now:

$$R_T = \frac{\alpha_T L}{EI} \quad R_B = \frac{\alpha_B L}{EI}$$

$$T_T = \frac{\beta_T L^3}{EI} \quad T_B = \frac{\beta_B L^3}{EI}$$

$$k = \sqrt{\frac{P}{EI}}$$

Solving the homogeneous deflection equation $v = A + Bz + C\sin kz + D\cos kz$ with the above boundary conditions results in the following determinant for the unknowns A, B, C and D.

$$\begin{vmatrix} T_T & (kL)^2 & 0 & T_T \\ 0 & R_T & R_T kL & (kL)^2 \\ T_B & \left[T_B - (kL)^2\right] & T_B \sin kL & T_B \cos kL \\ 0 & R_B & [R_B kL\cos kL - (kL)^2 \sin kL] & [-R_B kL\sin kL - (kL)^2 \cos kL] \end{vmatrix} = 0$$

13

The AISC Specification assumes that the top of the column is free to translate with respect to the bottom. Hence, the column is assumed to be fixed at the bottom which means $T_B = \infty$ and there is no translational restraint at the top i.e. $T_T = 0$. Using this, we can divide the third row of the above determinant by T_B and then insert the values of T_B and T_T. This gives us:

$$\begin{vmatrix} 1 & 0 & 0 & 1 \\ 0 & R_T & R_T kL & (kL)^2 \\ 1 & 1 & \sin kL & \cos kL \\ 0 & R_B & [R_B kL\cos kL - (kL)^2 \sin kL] & [-R_B kL\sin kL - (kL)^2 \cos kL] \end{vmatrix} = 0 \qquad \text{--2.24}$$

Also, the AISC specifications assumes that the beam bends in reverse curvature as shown in figure 11.
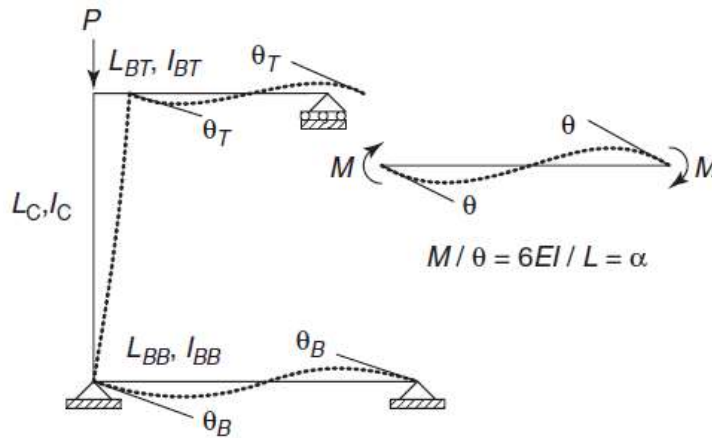
Figure 11 Sway permitted sub-assembly

Using figure 11, we can get to the following relationships:

$$\alpha_T = \frac{6EI_{BT}}{L_{BT}} \qquad \alpha_B = \frac{2EI_{BB}}{L_{BB}}$$

$$R_T = \frac{\alpha_T L_C}{EI_C} = \frac{6EI_{BT}}{L_{BT}} \text{X} \frac{L_C}{EI_C} = 6\left(\frac{\frac{I_{BT}}{L_{BT}}}{\frac{I_C}{L_C}}\right) = \frac{6}{G_T}$$

$$R_B = \frac{\alpha_B L_C}{EI_C} = \frac{6EI_{BB}}{L_{BB}} \text{X} \frac{L_C}{EI_C} = 6\left(\frac{\frac{I_{BB}}{L_{BB}}}{\frac{I_C}{L_C}}\right) = \frac{6}{G_B}$$

Where

$$G_T = \frac{\frac{I_C}{L_C}}{\frac{I_{BT}}{L_{BT}}} \qquad G_B = \frac{\frac{I_C}{L_C}}{\frac{I_{BB}}{L_{BB}}}$$

14

Evaluating the determinant in equation 2.24 and substituting the values of R_T and R_B, we get the following equation:

$$\frac{kL}{\tan kL} - \frac{(kL)^2 G_T G_B - 36}{6(G_T + G_B)} = 0 \qquad\qquad \text{--2.25}$$

Equation 2.25 is the basis for the alignment chart in AISC Specification for the sway permitted assembly.

2.2.4 Assumptions and Limitations

As evident from the previous sections, a number of assumptions were made while developing alignment charts. These assumptions are:

i. Elastic behavior.
ii. Reverse curvature bending of beams in sway case, and single curvature bending in non-sway case.
iii. Joints are rigid.
iv. Joint restraint is distributed to the columns above and below the joint proportional to I/L of the two columns.
v. All columns buckle simultaneously.
vi. No axial force in the girders.

Any frame that violates these assumptions cannot be analyzed using the alignment charts. Methods have been devised to account for these assumptions to some extent but it gets tedious to cater all the assumptions accurately. In addition to this, it can get fairly difficult to calculate the effective length factor for complex end restraints. Hence, the need arises to make us of other methods in order to accurately carry out the stability design of the structure. For the scope of this analysis, we will be restricting ourselves to the Direct Stiffness Method for stability analysis which will be discussed later.

2.3 Introduction to Nonlinear Analysis

Many structures behave in a linear elastic manner under the application of loading, however, there may be structures that exhibit some degree of nonlinearity. This nonlinearity may exist in the form of geometric and material nonlinearity which will be discussed in the following section. Due to the presence of these nonlinearities, a linear elastic analysis may not be able to accurately map the response of the structure under applied loads. These nonlinearities contribute additional stresses in the system and decrease its load carrying capacity. Mathematically, it is relatively difficult to carry out a nonlinear analysis which is why many engineers are not used to it. Unlike the case of linear elastic manner, where we get an exact solution for our structure, we have to rely on approximate solutions. Numerous methods have been   formulated for solving these nonlinear problems, with each method varying in its algorithm, complexity and suitability to a problem. As an engineer, one must have sufficient knowledge of these

solution techniques to better judge which is suitable for a given problem. Overall, nonlinear analysis presents a more accurate analytical simulation of the response of the structure.

2.3.1 Sources of Nonlinearity

As discussed before, nonlinearity may be in the form of geometric or material nonlinearity. When we perform a linear elastic analysis, we ignore the effect of these nonlinearities and that allows for simplification of the analysis. The simplification comes from the fact that we do not account for the deformation of the structure nor the yielding of the material. We will discuss the effect of accounting for these simplifying assumptions in the next section. For now, we will focus on the sources from which these nonlinearities originate.

2.3.1.1 Geometric Nonlinearity

The major source of geometric nonlinearity are the second order effects. There are two types of second order effects that can exist:

1. P△ effects:
   These refer to a destabilizing moment that is generated due to the horizontal sway of the structure. As the structure moves laterally, an additional moment is generated which is equal to the axial force times the lateral displacement.
2. Pδ effects:
   Recall we discussed in section 2.1.2 that due to the presence of initial imperfections, there is bending in the member prior to buckling. Due to this bending, an additional moment is generated which is equal to the axial force in the member times the member sway.

2.3.1.2 Material Nonlinearity

Presence of material nonlinearity in a structure nullifies the assumption that the material is unyielding and we have to take measures to account for that. There can exist multiple sources material nonlinearity in steel structures:

1. Plastic Deformations
2. Inelastic interaction of axial force, bending, shear, torsion

2.3.2 A Matrix Approach

For the scope of this project, we will be using a matrix approach or more specifically, the direct stiffness method to analyze our structure. British physicist Robert Hooke presented the Hooke's law in 1678 which forms the basis for direct stiffness method. According to Hooke's law:

$$F = kx$$

Hooke stated that stress applied is proportional to the strain produced in the elastic range where k is a constant i.e. stiffness of the material. We can modify Hooke's law in the form of matrices as:

$$\{F\} = [K]\{\triangle\}$$

By doing so, we solve a system of equations by relating the force vector to the displacement vector by the use of a stiffness matrix. In the linear elastic range, we use the elastic stiffness matrix and our equation becomes:

$$\{F\} = [K_e]\{\triangle\}$$

While incorporating geometric nonlinearity or the second order effects, we need to make use of the tangent stiffness matrix which is basically a sum of elastic and geometric stiffness components. Our equation takes the form:

$$\{F\} = [K_t]\{\triangle\}$$

$$\{F\} = [K_e + K_g]\{\triangle\}$$

Where K_g is the geometric stiffness matrix. For incorporating material nonlinearity, we have to make use of a plastic reduction matrix K_m which ensures that once a plastic hinge has formed at a member end, the force point at that end stays on the yield surface and it takes no further load. Our equation becomes:

$$\{F\} = [K_e + K_m]\{\triangle\}$$

If we want to account for both the material and geometric nonlinearity, we need to incorporate both the geometric stiffness matrix and the plastic reduction matrix along with the elastic stiffness component. Our equation then becomes:

$$\{F\} = [K_e + K_g + K_m]\{\triangle\}$$

The effect of these stiffness matrices on the analysis will be discussed in the next chapter and schemes will be presented for their solution.

3. Methodology

MATLAB Codes were prepared for different levels of analysis and results were compared with MASTAN2 for the verification studies. This section contains a detailed explanation of the algorithms for these analyses and the major operations involved in these algorithms. Flowcharts for all the analyses are attached in the appendix. Results will be presented in the next chapter. We will be assuming rigid connections and will neglect the effect of shear deformations in all the analyses. Assumptions specific to the analyses will be discussed in turn.

3.1 Critical Load Analysis

Critical buckling analysis is also termed as limit point analysis. Hence, we need to understand first what limit point is. As loads are applied to a structure, there comes a point after which any increase in loading will cause excessive deformations, resulting in a decrease in the load carrying capacity of the structure. This is known as the limit point. The structure is in a state of neutral equilibrium at the limit point and any increase in loading will cause the structure to become unstable. We know:

$$[K_t].\{\Delta\} = \{P\} \qquad \text{--3.1}$$

However, at the limit point, the right hand side of equation (i) becomes zero as there is no change in force for any change in the displacement. i.e.

$$[K_t].\{\Delta\} = 0 \qquad \text{--3.2}$$

The subscript 't' in the stiffness matrix denotes that it is the tangent stiffness matrix i.e. It is the sum of the elastic and geometric stiffness components. i.e.

$$[Ke + Kg].\{\Delta\} = 0 \qquad \text{--3.3}$$

As evident from equation 3.3, limit point will be achieved when both these stiffness matrices cancel each other out. Numerically, it is a point where the tangent stiffness matrix ceases to be positive definite i.e. after performing Gauss or Cholesky decomposition (Ref. 2), there exist one or more non-positive co-efficient on the main diagonal of the stiffness matrix. Another way of detecting the limit point is the appearance of one or more non-positive eigenvalues for the tangent stiffness matrix following the above mentioned decompositions.

3.1.1 Elastic Critical Load Analysis

For the elastic critical load analysis, we neglect the material non-linearity which allows for the assumption that the internal force distribution remains same at all ratios of the

applied loads. This assumption cancels the need for an incremental analysis and our task becomes simpler as we can apply the entire load in one step.

As we know, due to the aforementioned assumption, that all the elemental geometric stiffness matrices are linear functions of the axial forces present in those elements, we can modify equation 3.3 as:

$$[K_{e_{ff}} + \lambda K_{g_{ff}}].\{\Delta f\} = 0 \qquad \text{--3.4}$$

Or,

$$[K_{e_{ff}}].\{\Delta_f\} = \lambda [-K_{g_{ff}}]\{\Delta_f\} \qquad \text{--3.5}$$

The subscripts 'ff' denotes that only free degree of freedoms are considered, whereas λ is the critical load ratio. As evident from equation 3.5, λ gives us the value for which the elastic and geometric stiffness matrices cancel each other out. λ represents the ratio of the elastic critical load to the reference load.

Equation 3.5 is the general form of an eigenvalue problem. We will be using the power method to solve this eigenvalue problem but that requires for it to be first reduced to a standard form.

$$[H]\{Y\} = \omega\{Y\} \qquad \text{--3.6}$$

In order to obtain computational simplicity, it is desirable that [H] is a symmetric co-efficient matrix. Cholesky method (Ref. 2) was used for this purpose. The entire process of reducing the problem to the standard form is presented in Reference 3.

As mentioned above, we used power method to solve the eigenvalue problem. Other methods (Ref. 4) such as polynomial expansion or inverse iteration can also be used. Power method has a very simple algorithm and it starts with an initial guess {Y}, usually a vector of ones, substituted in left hand side of equation 3.6, giving,

$$[H]\{Y°\} = \{\hat{Y}^1\}$$

$\{\hat{Y}^1\}$ is then normalized to give,

$$\{Y^1\} = \{\hat{Y}^1\} / ||\hat{Y}^1||$$

The first approximation of the eigenvalue ω^1 is given by

$$\omega^1 = \{Y^1\}^T [H]\{Y^1\}$$

The process is repeated using $\{Y^1\}$ now to give better estimate of the eigenvalue. This process continues until convergence criteria is satisfied i.e.

$$\varepsilon_a < \text{tolerance}$$

Where,

$$\varepsilon_a = \frac{|\omega^i - \omega^{i-1}|}{|\omega^i|} * 100\%$$

3.1.2 Algorithm for Elastic Critical Load Analysis

From the input file, we read the geometry, node connectivity, material and section properties, applied loads and the boundary conditions. After we have initialized matrices, we proceed to the formulation of global elastic stiffness matrix, which is then used to find the displacements through which we can find internal forces in the elements. As the geometric stiffness matrix for an element in the function of axial force present in that element, we read the internal axial forces for each element to formulate the global geometric stiffness matrix. Once both the stiffness matrices have been populated, we read the rows and columns corresponding to free degree freedoms and can proceed to reduce it to the standard form of equation 3.6. After that, we make use of the power method as explained in section 3.1.1 to find the critical load ratio. This critical load ratio multiplied with the reference load gives us the elastic critical buckling load and we can plot the buckled configuration. Flowchart for the elastic critical load analysis is attached in the appendix.

3.1.3 Inelastic Critical Load Analysis

Until now, we have neglected the material non-linearity which, as discussed before, led to simplification of the analysis. However, we can add some degree of material non-linear behavior in the form of residual stresses.

The critical buckling load equation proposed by Euler is given as:

$$P_{cr} = \frac{\pi^2 EI}{L^2}$$

And the squash load is given by:

$$P_y = A\,\sigma_y$$

Slender or long columns are prone to buckling and short, stocky columns begin to fail by squashing. However, short columns can also buckle. The accepted explanation for this is the tangent modulus theory (Ref. 5). It is based on the inevitable presence of residual stresses in structural steel members due to non-uniform cooling during the manufacturing process. Due to the presence of these residual stresses, partial yielding takes place i.e. the material begins to yield (usually in the flanges) before we get to the yield point in the stress-strain diagram of the material. Due to this partial yielding, there

is a reduction in the stiffness of the material as our elastic modulus is decreasing. Hence, once yielding begins, we can no longer use the elastic modulus but have to use the tangent modulus to account for the loss of stiffness due to partial yielding. Galambos (Ref. 5) gave an empirical expression for the tangent modulus as:

$$E_t = 4E \left[\frac{\sigma}{\sigma y}\left(1 - \frac{\sigma}{\sigma y}\right)\right] \qquad \text{--3.7}$$

Where E_t is the tangent modulus, E is the elastic modulus, σ is the internal axial stress and σ_y is the yield stress. While elastic modulus is only a function of the type of material, the tangent modulus, as evident from equation 3.7, is also a function of the internal stress.

The next question is when to initiate the use of tangent modulus as partial yielding starts only after a specific amount of stress is applied and the elastic modulus gives the correct representation of the stiffness of the material before that load. Hence, for this purpose, we mark a proportional limit σ_p below the yield stress σ_y. This proportional limit dictates where to initiate the tangent modulus. Below the proportional limit, elastic modulus is to be used and once the internal stresses cross this proportional limit, tangent modulus comes into play.

Equation 3.7 comes with the assumption that the proportional limit is half the yield point i.e. when the internal stresses are greater than half the yield stress, elastic modulus is replaced by the tangent modulus.

As mentioned above, tangent modulus is not only a property of the material, but is also stress-dependent. Hence, now we cannot apply the entire loading in one load step but have to carry out an incremental analysis where we apply the load in steps, keeping a check of the internal stresses in a member. Once they exceed the proportional limit (0.5 σ_y in our case), E_t is to replace E and for every step after that, as the internal stresses change, E_t will also change.

As we now perform an incremental analysis, with the stiffness of the member subject to change due to the use of tangent modulus, the internal element forces and hence, the geometric stiffness matrix are no longer linear functions of the reference load as the internal force distribution is not the same for all load steps now.

Now, for an inelastic critical load analysis, we need to find the minimum load ratio $\overline{\lambda}$ that satisfies the following equation with $\lambda = 1$.

$$[K \, (\overline{\lambda} \, P_{ref})_{t,ff} + \lambda \, K(\overline{\lambda} \, P_{ref})_{g,ff}] \, \{\triangle_f\} = 0 \qquad \text{--3.8}$$

This was done by making use of regula falsi or false position method. But to be able to use regula falsi, we must have an equation of the form,

$$f(x) - 1 = 0 \qquad \text{--3.9}$$

We know from the equation 3.8 that both the stiffness matrices are the function of $\bar{\lambda} P_{ref}$ and λ must assume the value of 1. Hence we can manipulate equation 3.8 as:

$$[K (\bar{\lambda} P_{ref})_{bff} + \lambda K(\bar{\lambda} P_{ref})_{gff}] \{\triangle_f\} = 0$$

$$[K (\bar{\lambda} P_{ref})_{bff}] \{\triangle_f\} + \lambda K(\bar{\lambda} P_{ref})_{gff}] \{\triangle_f\} = 0$$

$$-[K (\bar{\lambda} P_{ref})_{bff}] \{\triangle_f\} = \lambda K(\bar{\lambda} P_{ref})_{gff}] \{\triangle_f\}$$

$$\lambda = -([K (\bar{\lambda} P_{ref})_{bff}] \{\triangle_f\}) (K(\bar{\lambda} P_{ref})_{gff}] \{\triangle_f\})^{-1} \qquad\qquad \text{--3.10}$$

Equation 3.10 suggests that RHS of it must be equal to 1 and hence can be used in place of f(x) in equation 3.9. As inelastic critical load will always be less than the elastic critical load, it is suggested that an elastic critical load analysis should be run and the elastic critical load should be used as a P_{ref} for equation 3.8. By doing so, we can be sure that $\bar{\lambda}$ has a value somewhere between 0 and 1 and they can be used as initial estimate for regula falsi.
Now, we have converted our problem into a simple root finding one and knowing the maximum and minimum values of $\bar{\lambda}$, we can perform iterations of regula falsi until RHS of equation 3.10 assumes a value of unity within a reasonable tolerance.

3.1.4 Algorithm for Inelastic Critical Load Analysis
After reading the input file and initializing matrices, we run the elastic critical load analysis to find the elastic critical load. We set the elastic critical load as the reference load in the light of the reasoning present in section 3.1.4. An elastic analysis is now run on this reference load to find the internal axial stresses in all elements. This helps us in determining whether elastic or inelastic buckling controls. If the internal axial stresses in all elements are less than half the yield stress, elastic buckling controls and the analysis is halted. However, if the internal axial stress in any element exceed the proportional limit, we proceed with the inelastic critical load analysis. Setting $\bar{\lambda}_{min}=0.001$ (not set zero as force vector becomes zero) and $\bar{\lambda}_{max}=1$, we can use equation 3.10 and equation 3.9 to initiate regula falsi to find the root i.e. the value of $\bar{\lambda}$ which satisfies equation 3.9. Of course, this value of $\bar{\lambda}$ will also satisfy equation 3.10 and when multiplied with the reference load (i.e. $\bar{\lambda} P_{ref}$), it gives us the inelastic critical buckling load. We can then plot the buckled configuration. Flowchart for the inelastic critical load analysis is attached in the appendix.

3.2 Load Deflection Analysis

While critical load analysis provides a good estimate of the limit state, it fails to offer any information about the post buckling behavior. In order to reasonably simulate the behavior of the structure, it is preferable to use the load deflection analysis. Although it uses relatively complex algorithms as compared to the critical load analysis, it provides a fairly accurate representation of the behavior of the structure. Different levels of load deflections analysis are presented in the succeeding sections with an insight into the merits and demerits of using these different analyses.

3.2.1 First Order Elastic Analysis

First order elastic analysis is the simplest of all the load-deflection analysis and is taught in most undergraduate programs. The simplicity of this analysis comes from the assumptions of neglecting both the material and geometric non-linearity. By neglecting material non-linearity, we assume the material to be of infinite yield strength i.e. it can never fail by yielding and by neglecting the geometric non-linearity, we make the equilibrium equation on the undeformed geometry. Owing to these assumptions, the stiffness matrix only consists of an elastic portion and the entire load can be applied in one step. Since there is no change in the stiffness of the structure, the load-deflection plot always shows a linear relationship. This analysis, however, is not suitable for structures where geometric and material non-linearity have a profound effect on the structure and thus, can't be ignored.

3.2.2 Algorithm for First Order Elastic Analysis

After reading the input file, we initialize matrices. We then assemble all the element stiffness matrices into a global stiffness matrix. Now that we have both the force vector and the stiffness matrix, we can find the deflection using,

$$\{\triangle\} = [K_e]^{-1} \{F\}$$

3.2.3 Second Order Elastic Analysis

As the name suggests, in this analysis, we do not ignore the second order effects but account for them. However, we are neglecting the material non-linearity and assuming the material to possess infinite yield strength. Second order or $P\triangle$ effects are prominent in high rise structures. Due to relatively large lateral displacements in such structures, the destabilizing moment generated by the axial forces, as the structure sways, cannot be neglected. Second order elastic analysis is similar to the elastic critical load analysis in the way that they use the same elastic and geometric stiffness matrices and both are failures of shape, however, this analysis gives a continuous response curve rather than a single point as in the case of elastic critical load analysis.

The main difference between first order and second order analysis is that in the first order analysis, equilibrium equations are formed on the undeformed configuration and in the second order analysis, equilibrium equations are formed on the deformed

configuration. Now, as the load is applied gradually, the geometry of the structure also changes gradually and hence, this suggests that loading maybe applied incrementally and the stiffness matrices may be updated at the end of each increment based on the new geometry of the structure.

This brings us to the two major operations involved in the analysis.

1. Updating Geometry:

As explained before, we formulate equilibrium equations on the new geometry or configuration after each increment. For this purpose, we need to update the geometry after each increment. A simple way of doing this is by adding the horizontal and vertical displacements of each node at the end of the load step, respectively, to the x and y co-ordinate of that node at the start of the load step.

2. Force Recovery:

Two types of the force recovery methods will be presented here.

    i.   Rigid Body Motion:

Figure 12 represents the orientation of an element and the forces associated with it at the beginning of a load increment. After the load increment, the element changes its orientation as shown in Figure 13. However, it must be noted that associated forces at the end of the load step are still oriented with the local axis of the element at the start of the load step. We need to make sure that the forces are oriented with the new local axis before we can proceed with the analysis. For this purpose, we make use of the transformation matrices. We will call the transformation matrix at the start of the step $[T^1]$ and the transformation matrix at the end of the load step $[T^2]$. What we essentially do is that we first bring the forces from the previous local axis to the global axis as,

$$\{F\}_{global\ axis} = [T^1]^T \{F\} \qquad\qquad \text{--3.11}$$

Once we have these forces aligned with the global axis, we then use $[T^2]$ to bring these forces to the new local axis as,

$$\{F\} = [T^2] \{F\}_{global\ axis} \qquad\qquad \text{--3.12}$$

This is an approximation to force recovery as it does not distinguish between the displacements resulting from rigid body motion and those due to deformations. It is suitable for structures with small strains and moderate displacements (Ref. 6), however, for highly non-linear structures, the following approach is preferable.

ii. Natural Deformations:

This approach, explained in Reference 7 distinguishes between the natural deformations due to stretching, flexure, etc and the rigid body motion. It assumes, that as an element rotates, the end forces associated with it rotate as well and there is no work required in this process, the forces remain unchanged. This also eliminates the need for transformation matrices. The only difference is that the displacement increments for any load step are replaced with natural displacement increments for that load step. The procedure for development of natural displacement is presented in Reference 7.
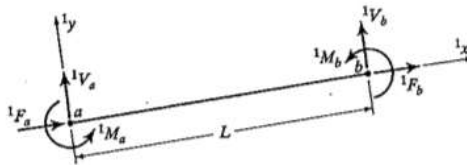
Figure 12 Element and forces orientation at start of load step
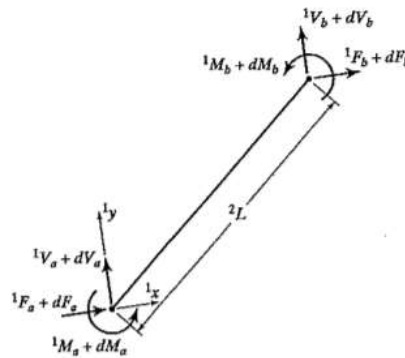
Figure 13 Orientation at end of load step before force recovery
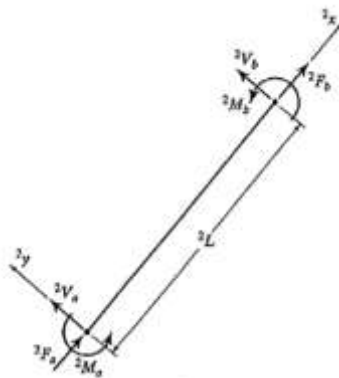
Figure 14 Orientation at end of load step after force recovery

Until now, we have discussed the formulation of non-linear equilibrium equations. The next step is to look for methods of solving these non-linear equations. These equations in an incremental analysis can be solved either by single-step or iterative procedures (Ref. 8). The iterative procedures are more accurate than the single-step methods as the generated response stays true to the actual equilibrium path whereas the single-step methods accumulate error due to the use of a single representative stiffness in each increment as shown in figure 15. This is called the drift-off error.
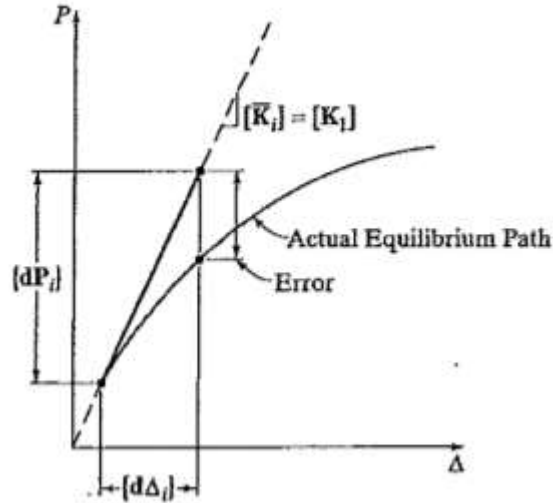
Figure 15 Drift-off error

One way of minimizing the drift-off error is the use of very small load steps, however that may require great computational effort for highly non-linear structures, hence it is more suitable to use automatic load increments as predefined load steps may not provide us with the accurate solution due to drift-off error. There are multiple schemes for automating the incremental loading. Reference 9 explains two of these. For our analysis, we make use of the current stiffness parameter presented s_i by Bergan et al. (Ref. 10) as,

$$s_i = \frac{[d\overline{\triangle_1}]^T \{P_{ref}\}}{[d\overline{\triangle_i}]^T \{P_{ref}\}} \qquad \text{----3.13}$$

Where s_i is the stiffness parameter, $d\overline{\triangle_1}$ are the incremental displacements for the first load step and $d\overline{\triangle_i}$ are the incremental displacements for the current load step. The stiffness matrix is basically a measure of the degree of non-linearity in the structure. Using this stiffness parameter, we can find the new load ratio for each step as,

$$d\lambda_i = \pm \ d\lambda_1 \ |s_i|^\Upsilon \qquad \text{--3.14}$$

Where $d\lambda_1$ is the load ratio at the start of the analysis. The exponent Υ is usually taken as 1, however, its value can vary between 0.5 and 1. 10-15% of the entire load is applied in the first step (Ref. 9). Due to the complex algorithms for the iterative procedures, we will stick to the single-step procedures.

Two strategies for incremental single-step analysis are explained below: -

Euler Method:

Euler method, or the simple step method is the most elementary single-step strategy. At the start of the analysis, equilibrium equations are formed on the undeformed geometry and the first load step is applied. At the end of the load step, the geometry is updated and force recovery methods are employed. So at the next step, equilibrium equations are formed based on this deformed geometry and the associated element forces. Similarly, for each load increment, stiffness is modified by forming the equilibrium based on the geometry and forces at the start of the increment.

Second-order Runge Kutta Method:

2nd order RK method is also known as the predictor-corrector method. It works by first applying half the load step and based on the deformed geometry and related forces, forms the stiffness matrix at the mid-point of the load step. Using this new updated stiffness matrix, the increment is repeated applying the entire load this time. Similarly, for each load step, we first find the stiffness matrix at the mid-point or half the load step with the predicted displacements or geometry associated with that load. This stiffness matrix is then used to find the corrected displacements or geometry for the entire load steps. Updating the geometry and force recovery operations are employed in a similar manner as in Euler method at the end of the corrector step i.e. at the end of the load increment.

3.2.4 Algorithm for Second Order Analysis

After reading the input file and initializing the matrices, we can employ either the Euler Method or the RK method to find the stiffness matrix for a load step. At the end of the load step, we update the geometry of the structure and perform force recovery using either the rigid body motion approach or the natural deformation approach. Also, at the end of each load step, we need to calculate the current stiffness parameter in order to update the load ratio for the next step. Once all this is done, we can proceed to the next load increment and repeat the same process until the stiffness matrix ceases to be positive definite.

3.2.5 First Order Inelastic Analysis

In both first order and second order elastic analysis, we assumed the material to have infinite yield strength and therefore, it could not fail by yielding. However, in the inelastic analysis, we do not make that assumption and material has a finite yield

strength. We will not be considering the second order effects for this analysis and the equilibrium equations are formulated on the undeformed geometry.

A hinge-by-hinge analysis will be carried out which consists of a series of elastic analysis with the member stiffness modified at the formation of a plastic hinge in that member. With the new, modified stiffness of the member, the elastic analysis is run again until another plastic hinge forms. This process is repeated until enough plastic hinges form to achieve the collapse mechanism.

Only the flexural hinges will be considered in the analysis. That is, to say, the axial and shear stresses do not contribute in the yielding process and only the flexural stresses caused by moments present at member ends dictate whether these member ends have yielded or not. We need to consider the moment-curvature plot of figure 16 for better understanding of flexural action.
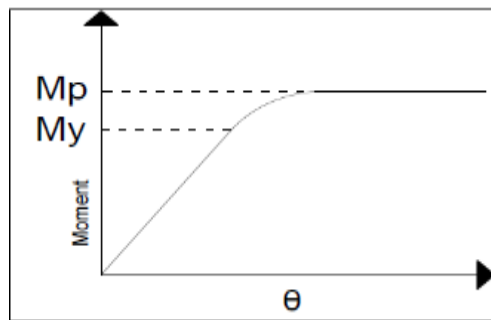
Figure 16 Moment curvature response
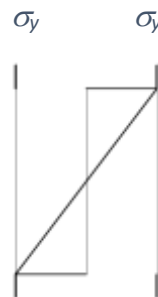
Figure 17 Stress profile at M$_y$

Figure 18 Stress profile at M$_p$

M_y is known as the yield moment and is the product of elastic section modulus and the yield stress. Figure 17 shows the stress distribution at a cross-section when moment attains the value of M_y. At this moment, the extreme fibers of the cross-section begin to yield and loss of stiffness is observed as we apply more moment, as can be seen in Figure 16. However, the entire cross-section has still not yielded and it can carry more load until we get to M_p, which is the plastic moment and is the product of the plastic section modulus and the yield strength. Figure 18 shows the stress distribution in the cross-section at M_p. it can be seen that the entire cross-section has now yielded and it can carry no further load as indicated by the flat-lining of the curve at M_p in fig(a). For the sake of our analysis, we neglect the partial yielding and hence, the non-linear response between M_y and M_p and assume the material to be perfectly elastic until M_p is reached, after which it becomes perfectly elastic. Figure 19 shows a comparison of the actual and assumed response.
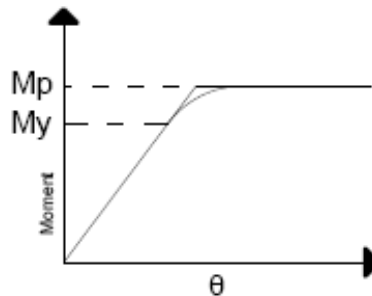
Figure 19 Assumed and actual moment curvature response

We will see later that the use of this model results in some complexities in the analysis and needs to be modified. However, before we get to that, we need to understand the analysis further.

We will be using the concentrated plasticity approach with the formation of zero-length plastic hinges. Of course, a more accurate response of plasticity can be achieved through the distributed plasticity theory. Another simplifying assumption is the use of plastic hinges rather than real hinges. The difference between the two being that real hinges carry no moment at all where plastic hinges will carry a moment equal to the plastic moment M_p of the member. Plastic hinges will take no additional moment after their formation, though still carrying M_p.

For our analysis, we assume that plastic hinges form only at the nodes and hence, for any member, there can only be four cases: -

1. A member without hinges
2. A member with a left end hinge
3. A member with a right end hinge
4. A member with hinges at both ends

The only difference for all these cases is the use of a different member stiffness matrix. The stiffness matrices for all the cases are presented in figure 20. The reader is referred to Reference 11 for the study of development of these matrices.

$$\begin{bmatrix} \frac{EA}{L} & 0 & 0 & -\frac{EA}{L} & 0 & 0 \\ 0 & \frac{12EI}{L^3} & \frac{6EI}{L^2} & 0 & \frac{-12EI}{L^3} & \frac{6EI}{L^2} \\ 0 & \frac{6EI}{L^2} & \frac{4EI}{L} & 0 & -\frac{6EI}{L^2} & \frac{2EI}{L} \\ -\frac{EA}{L} & 0 & 0 & \frac{EA}{L} & 0 & 0 \\ 0 & -\frac{12EI}{L^3} & -\frac{6EI}{L^2} & 0 & \frac{12EI}{L^3} & -\frac{6EI}{L^2} \\ 0 & \frac{6EI}{L^2} & \frac{2EI}{L} & 0 & -\frac{6EI}{L^2} & \frac{4EI}{L} \end{bmatrix} \qquad \begin{bmatrix} \frac{EA}{L} & 0 & 0 & -\frac{EA}{L} & 0 & 0 \\ 0 & \frac{3EI}{L^3} & 0 & 0 & -\frac{3EI}{L^3} & \frac{3EI}{L^2} \\ 0 & 0 & 0 & 0 & 0 & 0 \\ -\frac{EA}{L} & 0 & 0 & \frac{EA}{L} & 0 & 0 \\ 0 & -\frac{3EI}{L^3} & 0 & 0 & \frac{3EI}{L^3} & -\frac{3EI}{L^2} \\ 0 & \frac{3EI}{L^2} & 0 & 0 & -\frac{3EI}{L^2} & \frac{3EI}{L} \end{bmatrix}$$

CASE 1   **CASE 2**

$$\begin{bmatrix} \frac{AE}{L} & 0 & 0 & -\frac{AE}{L} & 0 & 0 \\ 0 & \frac{3EI}{L^3} & \frac{3EI}{L^2} & 0 & -\frac{3EI}{L^2} & 0 \\ 0 & \frac{3EI}{L^2} & \frac{3EI}{L^2} & 0 & -\frac{3EI}{L^3} & 0 \\ -\frac{AE}{L} & 0 & 0 & \frac{AE}{L} & 0 & 0 \\ 0 & -\frac{3EI}{L^3} & -\frac{3EI}{L^2} & 0 & \frac{3EI}{L^3} & 0 \\ 0 & 0 & 0 & 0 & 0 & 0 \end{bmatrix} \qquad \begin{bmatrix} \frac{EA}{L} & 0 & 0 & -\frac{EA}{L} & 0 & 0 \\ 0 & 0 & 0 & 0 & 0 & 0 \\ 0 & 0 & 0 & 0 & 0 & 0 \\ -\frac{EA}{L} & 0 & 0 & \frac{EA}{L} & 0 & 0 \\ 0 & 0 & 0 & 0 & 0 & 0 \\ 0 & 0 & 0 & 0 & 0 & 0 \end{bmatrix}$$

CASE 3   **CASE 4**

Figure 20 Stiffness matrices for different cases of plastic hinge formation

For the case 1 where no plastic hinges have formed in the member, the stiffness matrix is same as the elastic stiffness matrix which we have used in the previous analysis. For case 2, as the plastic hinge forms at the left end or left node of the member, it can be seen that the third row and third column only contains zeros. The third row and column corresponds to the flexural stiffness at the left end and the presence of zeros indicates that the member can now take no further moment. In the force vector, the third element corresponds to the moment at the left end and its value will now be zero. Similarly, for case 3, the sixth row and column are zero.

It is observed that if all the member ends connected to a specific node have formed a plastic hinge, the row and column corresponding, in the global degree of freedom, to the moment at that node in the global stiffness matrix, become zero. It is a property of matrices that if an entire row or column of a matrix is zero, the matrix becomes singular and the inverse of a singular matrix does not exist. For our analysis, we need to take the inverse of the stiffness matrix, hence, we need to find a way to avoid this. This tells us

that we cannot rely on the use of the elastic perfectly plastic model derived before if we want to avoid this local joint instability. We will restrict ourselves to the use of a linear elastic linear strain hardening model in which we use an elastic element of a relatively small stiffness in parallel to any elements with yielded ends. So, our moment-curvature response at the cross-sectional level becomes that of figure 21.
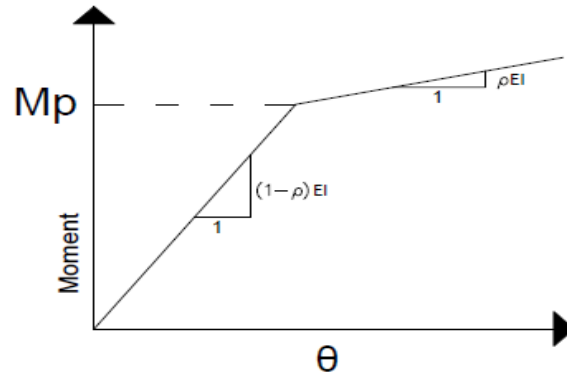
Figure 21 Elastic linear strain hardening moment curvature response

Note that we are still neglecting the partial yielding and assuming a linear elastic response up till M_p. ρ is the hardening parameter and usually has a very small value. What we basically do is that we decompose the response by using two stiffness matrices i.e.

$$K_1 = \rho \, K_e \qquad K_2 = (1\text{-}\rho) \, K_e$$

$$K_{total} = K_1 + K_2$$

While the material has not yielded at any end, the addition of two stiffness matrices will cancel out the hardening parameter, and K_{total} will be equal to K_e. For K_1, K_e from case 1 is always used as it represents the linear strain hardening by reducing the elastic stiffness through the use of the hardening parameter whereas of K_2, K_e can vary between all the four cases based on the formation of plastic hinges.

3.2.6 Algorithm for First Order Inelastic Analysis
After reading the input file and initializing matrices, we formulate appropriate stiffness matrices for each element based on the formation of plastic hinges in the element. We then form the global stiffness matrix and find the incremental displacements. These displacements are used to find incremental internal moments at each element end. Also, at each element end, a scale factor is calculated by dividing the "remaining plastic capacity" at the end by the plastic moment of the member. The minimum of all these scale factors is chosen as the governing scale factor and the incremental forces and the displacements are amplified by multiplying with this scale factor. If excessive displacements are encountered, it indicates collapse and the process is halted. Otherwise, the internal forces and displacement arrays are updated and the entire

process is repeated until the structure collapses. All the governing scale factors are added to give the total scale factor. It should be noted that loads are to be applied as a ratio of the actual loading.

3.2.7 Second Order Inelastic Analysis

The second order inelastic analysis takes both material and geometric non-linearity into account. It is the most accurate of all the analysis. It takes into account the second order effects, while also assuming the material to have a finite yield strength. It basically combines the operations presented in section 3.2.3 and 3.2.5.

3.2.8 Algorithm for Second Order Inelastic Analysis

An incremental analysis is applied similar to the case of second order elastic analysis while keeping check for the internal moments. Updating of geometry, force recovery and calculation of stiffness parameter to obtain the next load ratio is done in the same manner as before at the end of each step. However, if a plastic hinge forms between a load step, we make use of regular falsi to find the load ratio for which the plastic hinge would form at the end of the step. Now, the load step is repeated using the new load ratio to ensure the formation of plastic hinge at the end of the step so that the next load step can be applied with the modified stiffness of the elements in which the plastic hinge forms.

4. Results

We will present the results from our MATLAB codes in this section and verify them. We will also be comparing the critical load analysis with alignment charts and the determinant approach.

4.1 Elastic Critical Load Analysis

We ran the elastic critical load analysis for three example frames and results were identical to those from MASTAN2 with less than 1% error.

Applied Load Ratio = 724646.8659

7.246671307078463e+05

Critical Load=**724 Kips**

ξ < 1%

Critical Load=**724 Kips**
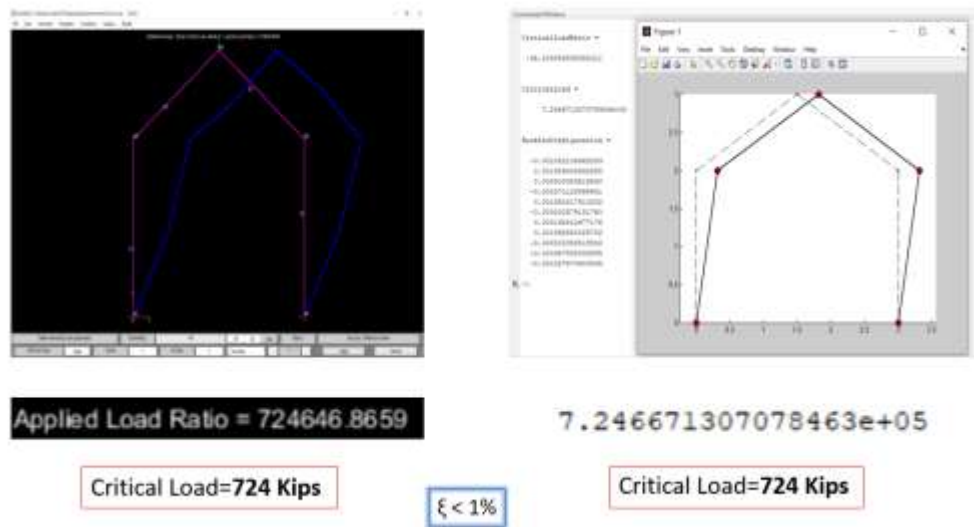
Figure 22 Elastic critical load example 1

Applied Load Ratio = 885038.4136

8.851069518765865e+05

Critical Load=**885 Kips**

ξ < 1%

Critical Load=**885 Kips**
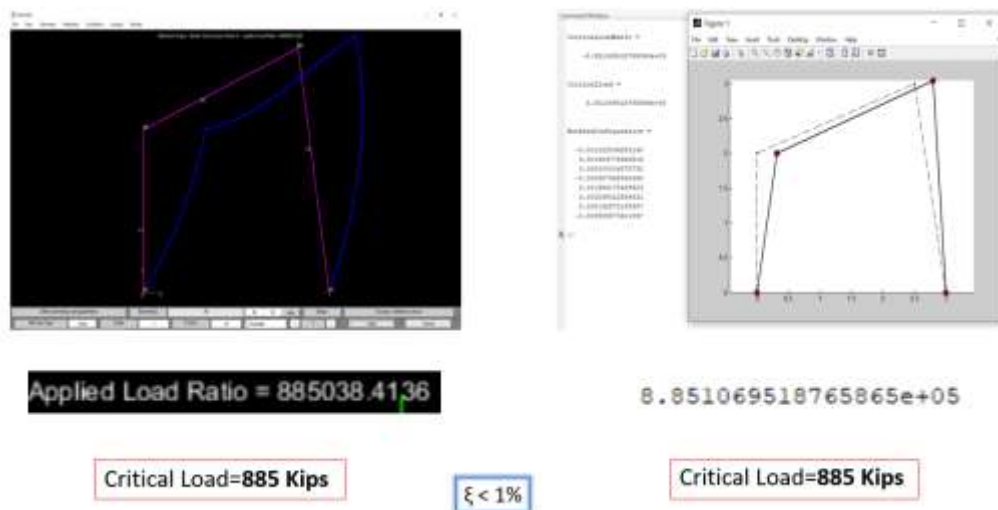
Figure 23 Elastic critical load example 2

Applied Load Ratio = 2263491.4195

2.280455557797884e+06

Critical Load=**2263 Kips**

ξ < 1%

Critical Load=**2280 Kips**
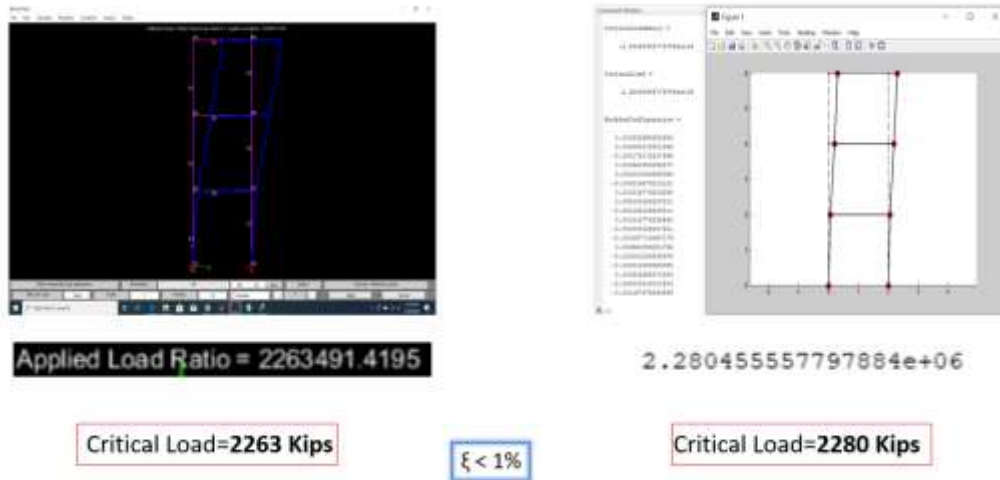
Figure 24 Elastic critical load example 3

4.2 Inelastic Critical Load Analysis

Similarly, we ran the inelastic critical load analysis on three reference frames with a finite yield strength. The results were identical to those from MASTAN2 and the error was less than 1% in all cases.

Inelastic Critical Load, Mode # 1, Applied Load Ratio = 673660.116

Inelastic Critical Buckling Load = 673576.2177

Critical Load=**673 Kips**

ξ < 1%

Critical Load=**673 Kips**
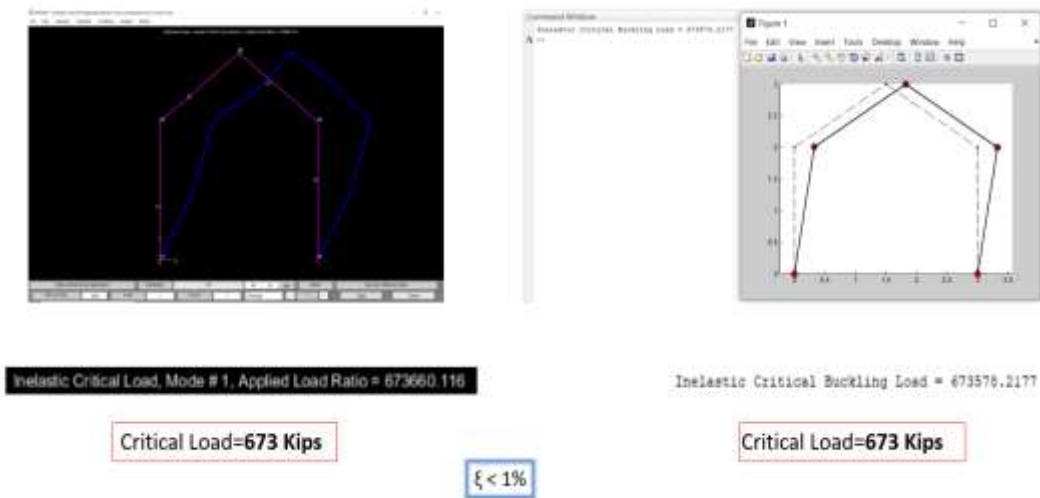
Figure 25 Inelastic critical load example 1

Critical Load=**385 Kips**

Critical Load=**385 Kips**

ξ < 1%

Figure 26 Inelastic critical load example 2

Critical Load=**2219 Kips**

Critical Load=**2219 Kips**

ξ < 1%

Figure 27 Inelastic Critical Load Example 3

4.3 Second Order Elastic Analysis

MATLAB codes were developed for both Euler method and the 2nd order RK method using both the rigid body motion approach and the natural deformations approach for the force recovery process. It can be seen in figure 29 and figure 30 that natural deformations approach can more accurately map the response of the structure when it becomes highly nonlinear.
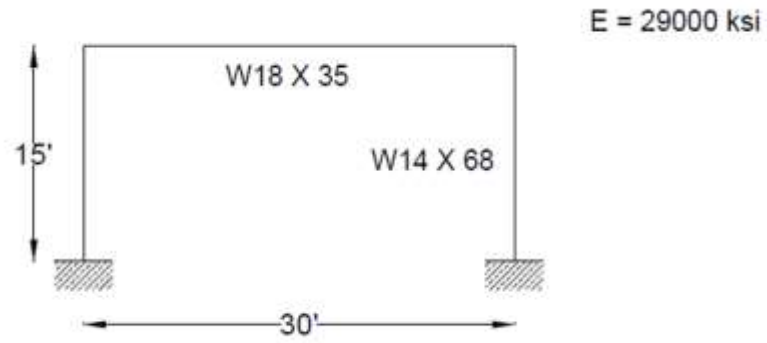
Figure 28 Example single bay frame

4.3.1 Euler Method

Rigid Body Motion

Natural Deformations
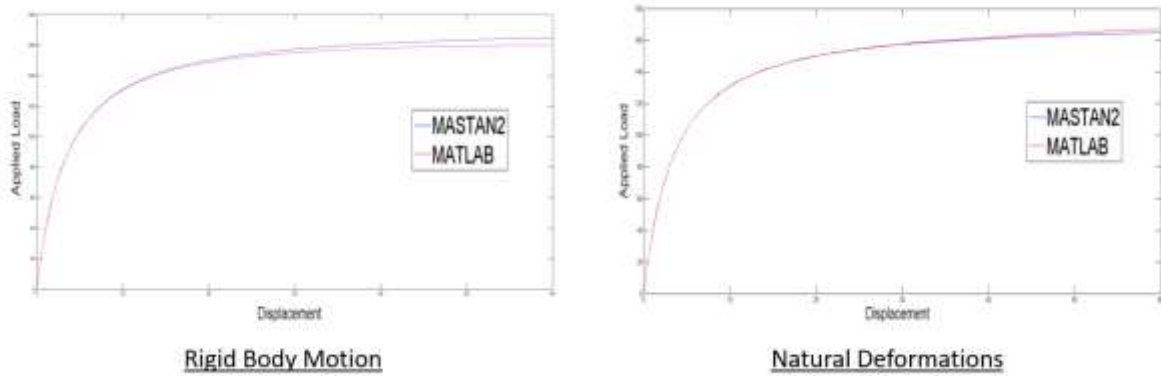
Figure 29 Comparison of results between MATLAB and MASTAN2 for Euler Method

4.3.2 2nd Order RK Method

Rigid Body Motion

Natural Deformations
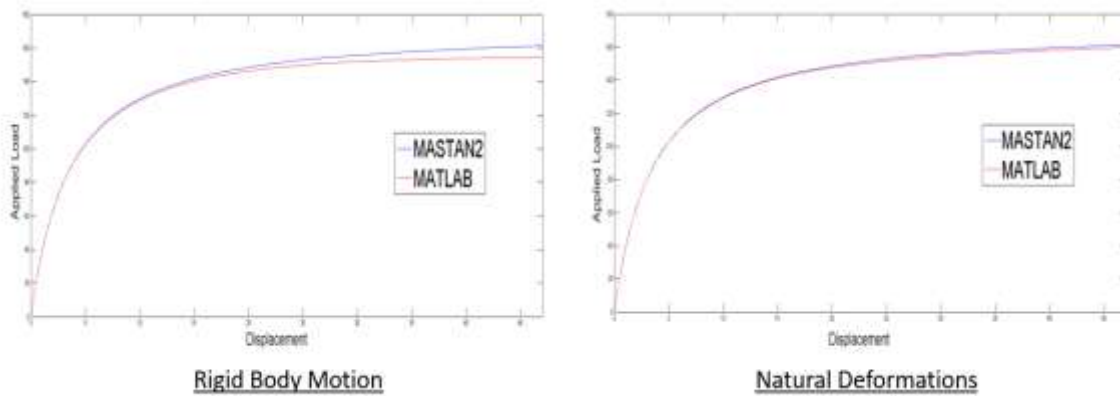
Figure 30 Comparison of results between MATLAB and MASTAN2 for RK Method

4.4 First Order Inelastic Analysis

For the first order inelastic analysis, we could not compare our results with MASTAN2 as it also accounts for the role of axial force in the yielding process making use of a yield surface to check whether a plastic hinge forms or not. It also uses the plastic reduction matrix to ensure that once plastic hinge has formed, the force point does not drift off from the yield surface. Whereas, we are only considering flexural hinges so we will compare our results with two examples presented in Reference 11. Total scale factors from Reference 11 and our MATLAB codes came out to be the same. Load deflection plots for the top node are also attached.

Figure 31 Example 1

Figure 32 MATLAB scale factor result
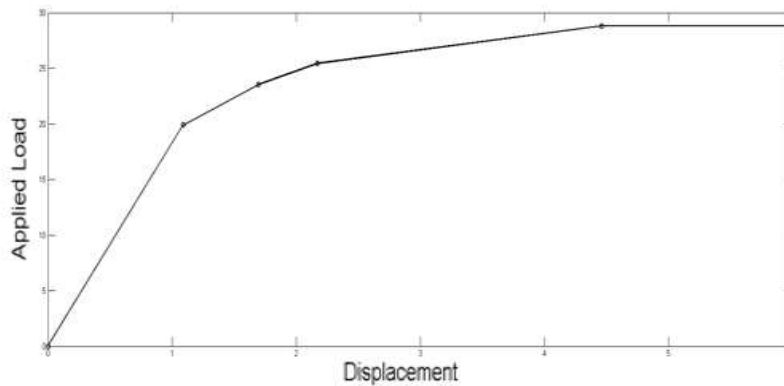
Figure 33 Load deflection plot for node 2
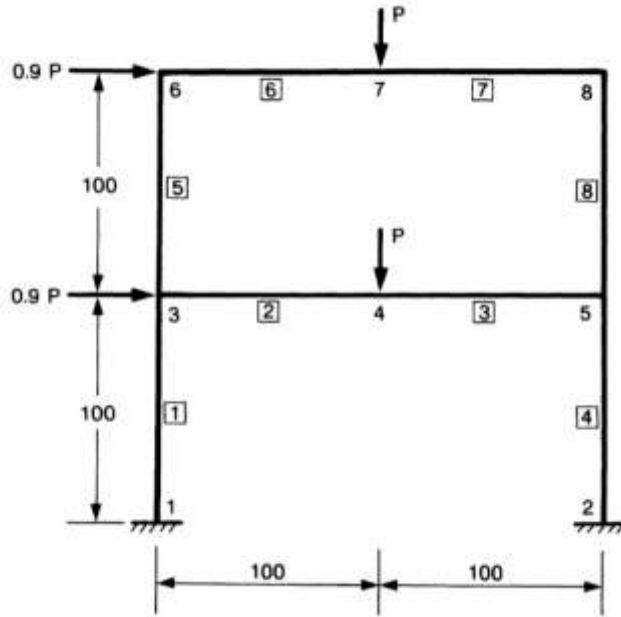
Figure 34 Example 2

```
collapse imminent
Total_Scale_Factor =
    63.0641
```

Figure 35 MATLAB scale factor result
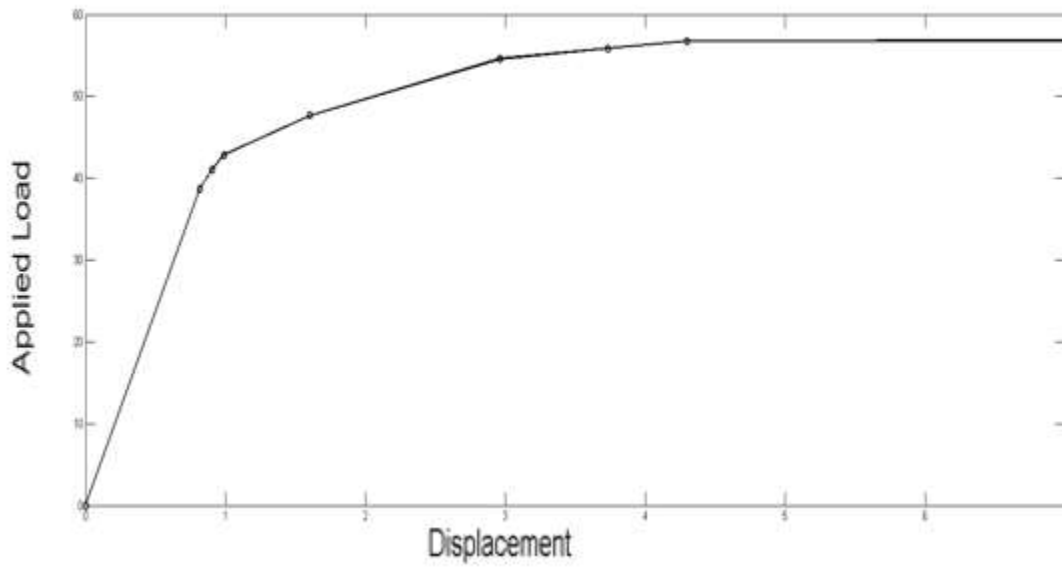
Figure 36 Load deflection plot for node 6

4.5 Comparison of Load Deflection Analyses

Figure 37 shows a comparison of the different levels of load deflection analysis for the example single bay frame shown in figure 28. Of course, the results for inelastic analyses are not correct as we are only considering flexural hinges but this is only to show what all these analyses look like when compared to each other.
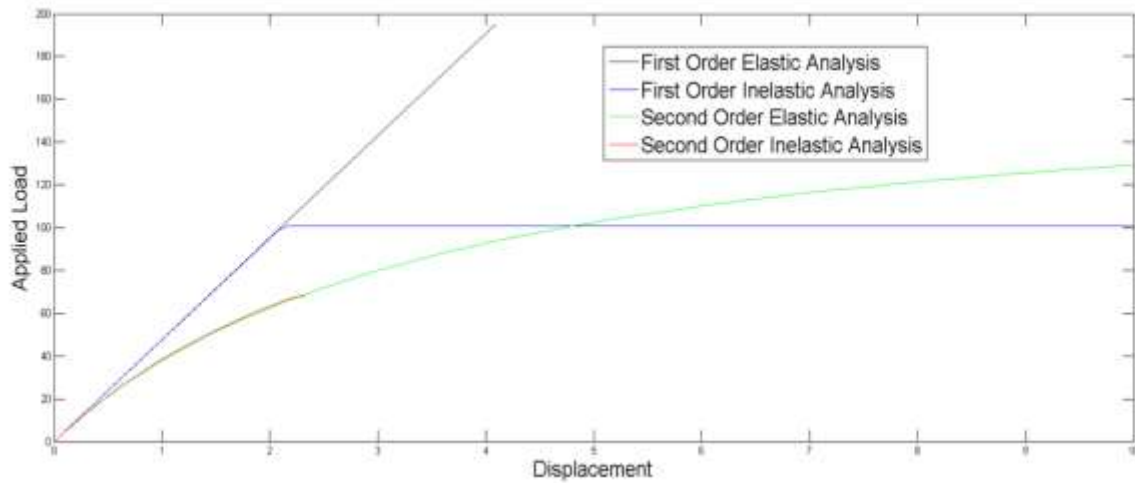
Figure 37 Comparison of load deflection analyses

4.6 Comparison of Element Subdivision

In the critical load analysis, we may need to subdivide our elements in order to achieve accurate results. The table below shows a comparison of the theoretical critical load values for some fundamental boundary conditions and the analytical results from MATLAB codes for the critical load analysis. We can see that we need to divide our element into at least 4 sub elements in order to get accurate results. Consider a column with following properties:

W14x82
L= 40 ft
A= 24 in^2
I= 881 in^4
E=29000 ksi

pinned—pinned			
# of elements	Theoretical P_{cr}	Analysis P_{cr}	% difference
1	1094.4	1330.37	21.56
2	1094.4	1102.7	0.76
4	1094.4	1095	0.05
8	1094.4	1094.5	0.009
16	1094.4	1094.4	0

fixed—pinned			
# of elements	Theoretical P_{cr}	Analysis P_{cr}	% difference
1	2233.5	3326.7	48.94
2	2233.5	2296.4	2.82
4	2233.5	2243.5	0.45
8	2233.5	2239.3	0.26
16	2233.5	2239	0.25

fixed—fixed			
# of elements	Theoretical P_{cr}	Analysis P_{cr}	% difference
1	4377.8	696000	15798
2	4377.8	4435.6	1.32
4	4377.8	4410.7	0.75
8	4377.8	4380	0.05
16	4377.8	4377.9	0.002

fixed—free			
# of elements	Theoretical P_{cr}	Analysis P_{cr}	% difference
1	273.61	275.7	0.76
2	273.61	273.75	0.05
4	273.61	273.62	0.004
8	273.61	273.61	0
16	273.61	273.61	0

4.7 Comparison of Residual Stress with Modulus

So far, we have discussed two ways of calculating the effect of residual stresses on modulus of the material. Section 2.1.3.1 presents a way of doing so based on the individual residual stress profile of the material whereas equation 3.7 presents an analytical approach. The comparison of two for the same numerical example of section 2.1.3.1 is shown in figure 38. It can be seen that there is some variation between the curves for both cases. This is mainly due the assumption that equation 3.7 makes where it sets the proportional limit to half the yield strength. However, as we saw in the numerical example, our material only remained elastic until 12 ksi (~28% of yield strength). The approach for calculating the modulus based on the actual residual stress profile can be made more accurate by using a cubic response for the stress rather than a quadratic one as we used. However, doing so would require another boundary condition.
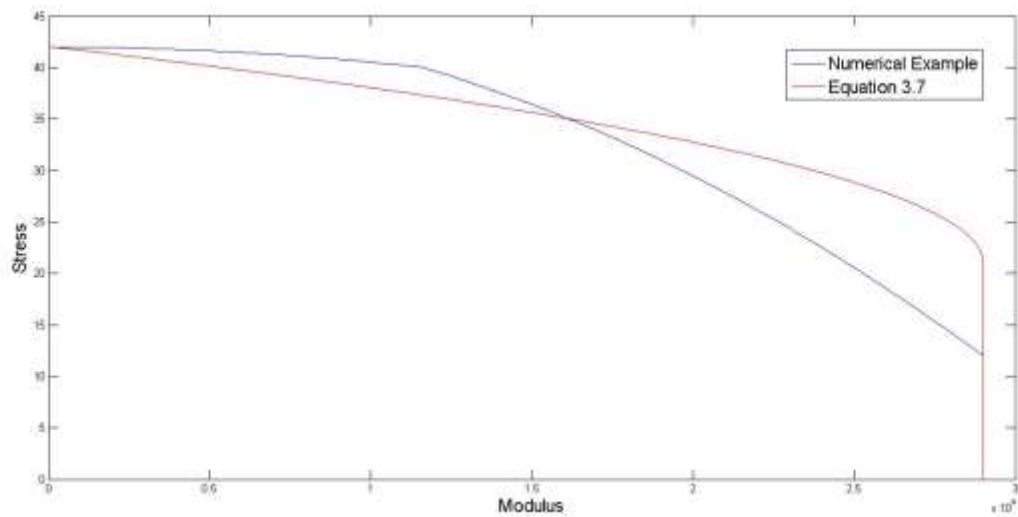
Figure 38 Residual Stress Comparison

4.8 Different Approaches to Find the Critical Load

We will compare the different approaches of finding the critical load for the example frame shown in figure 39. We will do so by comparing the effective length factors for each approach.
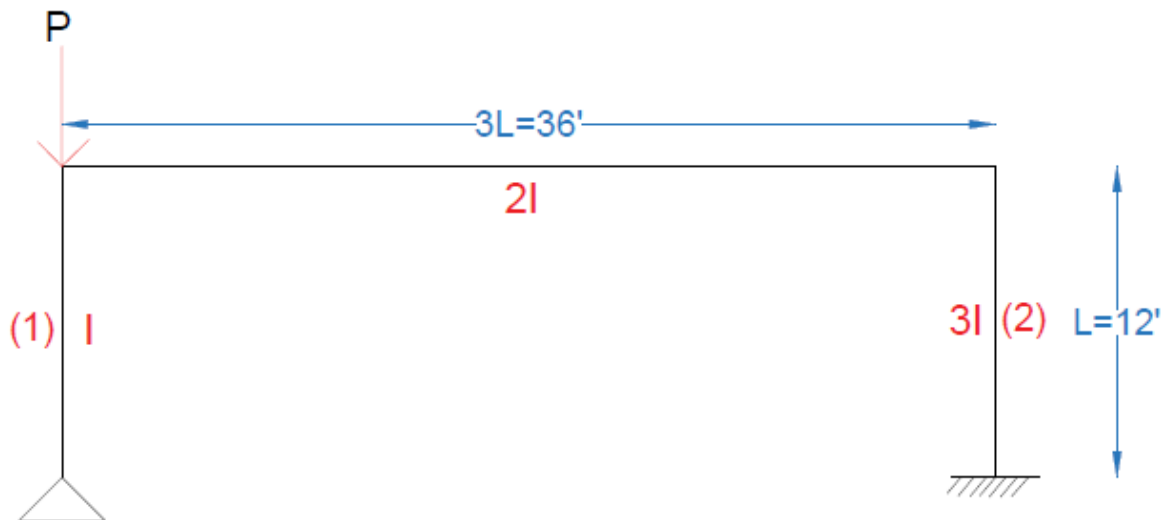
Figure 39 Example frame

4.8.1 Determinant Approach

For the determinant approach, we will follow the same principle presented in section 2.2.3. The rotational and translational spring constants in this case are:

$$\alpha_T = \frac{40EI}{17L} = \frac{40EI}{17X12} = 0.19608EI$$

$$\beta_T = \frac{90EI}{7L^3} = \frac{90EI}{7X(12)^3} = 0.00744EI$$

Now we will calculate the restrain factors at the top and bottom of the column 1.

$$R_T = \frac{\alpha_T L}{EI} => \frac{0.19608EI(12)}{EI} => 2.35296$$

$$T_T = \frac{\beta_T L^3}{EI} => \frac{0.00744EI(12)^3}{EI} => 12.85632$$

The restrain factors at the bottom of the column would be $R_B = 0$ and $T_B = \infty$. We also know from section 2.2.3 that the determinant for such a scenario would have the following form:

$$\begin{bmatrix} T_T & (kL)^2 & 0 & T_T \\ 0 & R_T & R_T kL & (kL)^2 \\ 1 & 1 & \sin kL & \cos kL \\ 0 & 0 & -(kL)^2 \sin kL & -(kL)^2 \cos kL \end{bmatrix} = 0$$

Solving the determinant results in:

$$T_T R_T(kL) - T_T(kL)^2 \tan kL - R_T(kL)^3 + (kL)^4 \tan kL - T_T R_T \tan kL = 0$$

Now substituting values of T_T and R_T in above equation:

$$30.25kL - 12.856(kL)^2 \tan kL - 2.353(kL)^3 + (kL)^4 \tan kL - 30.25 \tan kL = 0$$

$$[(kL)^4 - 12.856(kL)^2 - 30.250] \tan kL - kL(2.353(kL)^2 - 30.25) = 0$$

The above equation was solved in MATLAB using a root finder approach. It works by assigning an array of values to kL and evaluating the function for each kL value. It stores the value of kL for which the function changes sign, as that indicates the root of the function. The effective length factor K was then calculated by:

$$K = \frac{\pi^2}{kL}$$

Which came out to be:

$$K = 0.93$$

4.8.2 Alignment Charts
For the alignment charts, all we need are G_T and G_B factors. For our example frame, they are:

$$G_T = \frac{I_{cT}/L_{cT}}{I_{BT}/L_{BT}} = \frac{I/12}{2I/36} = 1.5$$

$$G_B = \frac{I_{cB}/L_{cB}}{I_{BB}/L_{BB}} = \frac{I/12}{0/0} = \infty$$

We then make use of alignment charts are shown in figure 40 to find the effective length factor which comes out to be:

$$K = 2.5$$
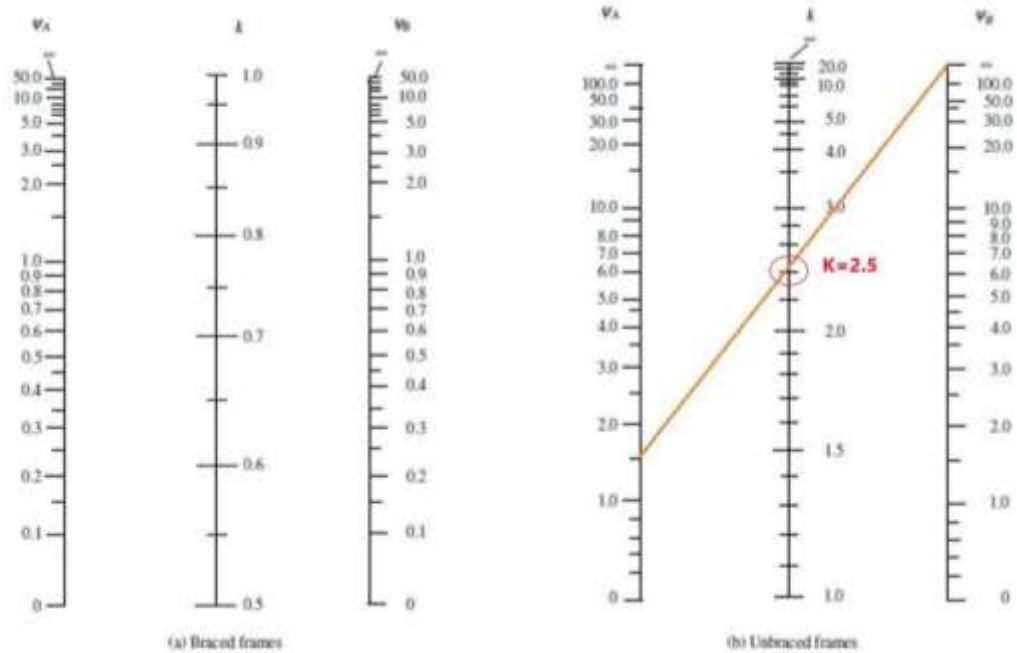
Figure 40 Effective length factor through alignment charts

4.8.3 Critical Load Analysis

The same example frame was solved using the elastic critical load analysis program in MATLAB. The columns were divided into 8 sub elements in order to get accurate results in light of the results presented in section 4.6. Critical load was calculated and then the effective length factor was calculated. We know that:

$$P_E = \frac{\pi^2 EI}{(KL)^2}$$

So we can calculate the effective length factor as:

$$K = \frac{\pi}{L}\sqrt{\frac{EI}{P_E}}$$

Which comes out to be:

$$K = 0.95$$

4.8.4 Comparison

As can be seen, using alignment charts results in in accuracy. This is due to the fact that this example frame violates the assumptions of alignment charts mentioned in section 2.2.4. Using alignment charts, we ignore the lateral restraint and only consider the rotational restraint. This results in incorrect solution as lateral restraint plays a crucial role in the buckling process. Determinant approach serves as an accurate way of finding the critical load but it can get tedious for a relatively larger frames as we would have to find the boundary conditions to solve the determinants. Critical load analysis not only provides an accurate solution, but also eases the job of the analyst. All one has to do is model the entire frame assembly and run the analysis using the procedures presented in section 3.1.1 and 3.1.2. Inelastic behavior can also be accounted for using section 3.1.3 and 3.1.4.

5. Discussion and Conclusion

Results for our MATLAB codes have been verified and the flowcharts attached in the appendix show the structure of the program. To our knowledge, there does not exist any work in previous literature that contains these analyses, their explanations and their flowcharts all in one place. Many new researchers are unsure about where to start and we believe that this work will be a good place to start for anyone who is willing to get into research in any area of structural stability. We believe our work is in easy to understand language which will be very beneficial to students in grasping the concepts of the subject. Our work will open doorways for the students to pursue further research in structural stability. Also, it encourages the students to become proficient in the use of computational software and to use them in practical problem solving. We would like to recommend that our MATLAB codes should be used for teaching purposes as it is nearly impossible to carry out nonlinear analysis by hand and doing so would set the students at ease with computational platforms which is a necessity in this time and age.

The direct analysis method presented in AISC 360 is the state of the art method for stability analysis. It makes use of two moment amplification factors, B1 and B2, to account for the role of second order effects in stability of the structure. B1 factor caters for the additional moment due to member sway (Pδ effect) and B2 factor accounts for the additional moment due to horizontal sway of the structure (PΔ effect). However, according to the AISC Specification, if B2 is greater than 1.5 (while using reduced stiffness for elements) or 1.7 (while using actual stiffness), then this indicates that second order effects are significant and one must perform a rigorous second order analysis. While many design engineers have now developed adequate understanding of the direct analysis method, many are reluctant to the use of rigorous second order analysis as they cannot completely comprehend it. We believe that our work will serve to develop a sound understanding of the rigorous second order analysis and will aid the design engineers by familiarizing them with its use. There are multiple commercially available software that provide embedded second order facility but they are merely tools and can only be used effectively if the engineer has a good idea of what's happening in the backend of those software.

6. References

1. Theodore V. Galambos, and Andrea E. Suvorek, *Structural Stability of Steel: Concepts and Applications for Structural Engineers,* John Wiley and Sons, 2008, pg. 43-51.

2. William McGuire, Richard H. Gallagher and Ronald D. Ziemian, *Matrix Structural Analysis, Second Edition,* John Wiley and Sons, 2000, pg. 302-309.

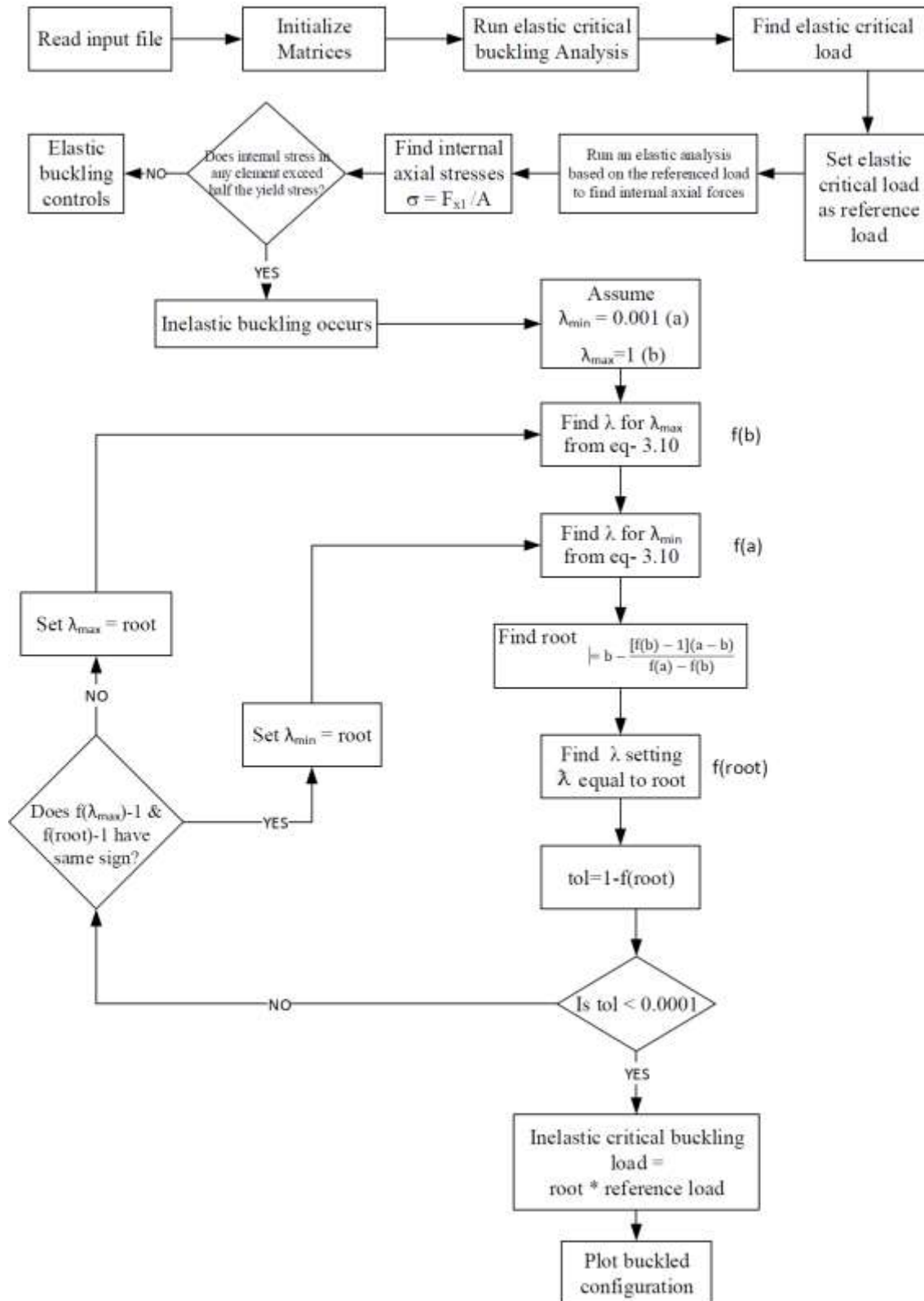3. William McGuire, Richard H. Gallagher and Ronald D. Ziemian, *Matrix Structural Analysis, Second Edition,* John Wiley and Sons, 2000, pg. 361-363.

4. William McGuire, Richard H. Gallagher and Ronald D. Ziemian, *Matrix Structural Analysis, Second Edition,* John Wiley and Sons, 2000, pg. 363-369.

5. T. V. Galambos, editor, John Wiley and Sons, *Guide to Stability Design Criteria for Metal Structures*, 5th edition, New York, 1998.

6. William McGuire, Richard H. Gallagher and Ronald D. Ziemian, *Matrix Structural Analysis, Second Edition,* John Wiley and Sons, 2000, pg. 352-355.

7. William McGuire, Richard H. Gallagher and Ronald D. Ziemian, *Matrix Structural Analysis, Second Edition,* John Wiley and Sons, 2000, pg. 444-450.

8. William McGuire, Richard H. Gallagher and Ronald D. Ziemian, *Matrix Structural Analysis, Second Edition,* John Wiley and Sons, 2000, pg. 340-351.

9. William McGuire, Richard H. Gallagher and Ronald D. Ziemian, *Matrix Structural Analysis, Second Edition,* John Wiley and Sons, 2000, pg. 351-352.

10. P. G. Bergan, G. Horrigmoe, B. Krakeland, and T.H. Søreide, "Solution Techniques for Nonlinear Finite Element Problems," *Intl. Jl. Num. Meth. In Engr.,* Vol. 12, 1978, pg. 1677-1696.

11. W. F. Chen, and I. Sohal, *Plastic Design and Second Order Analysis of Steel Frames,* Springer-Verlag, 1995, pg. 381-415.

12. M. J. Clarke, and G. J. Hancock, "A Study of Incremental-Iterative Strategies for Nonlinear Analyses", *Intl. Jl. Num. Meth. In Engr.,* Vol. 29, 1990, pg. 1365-1391.
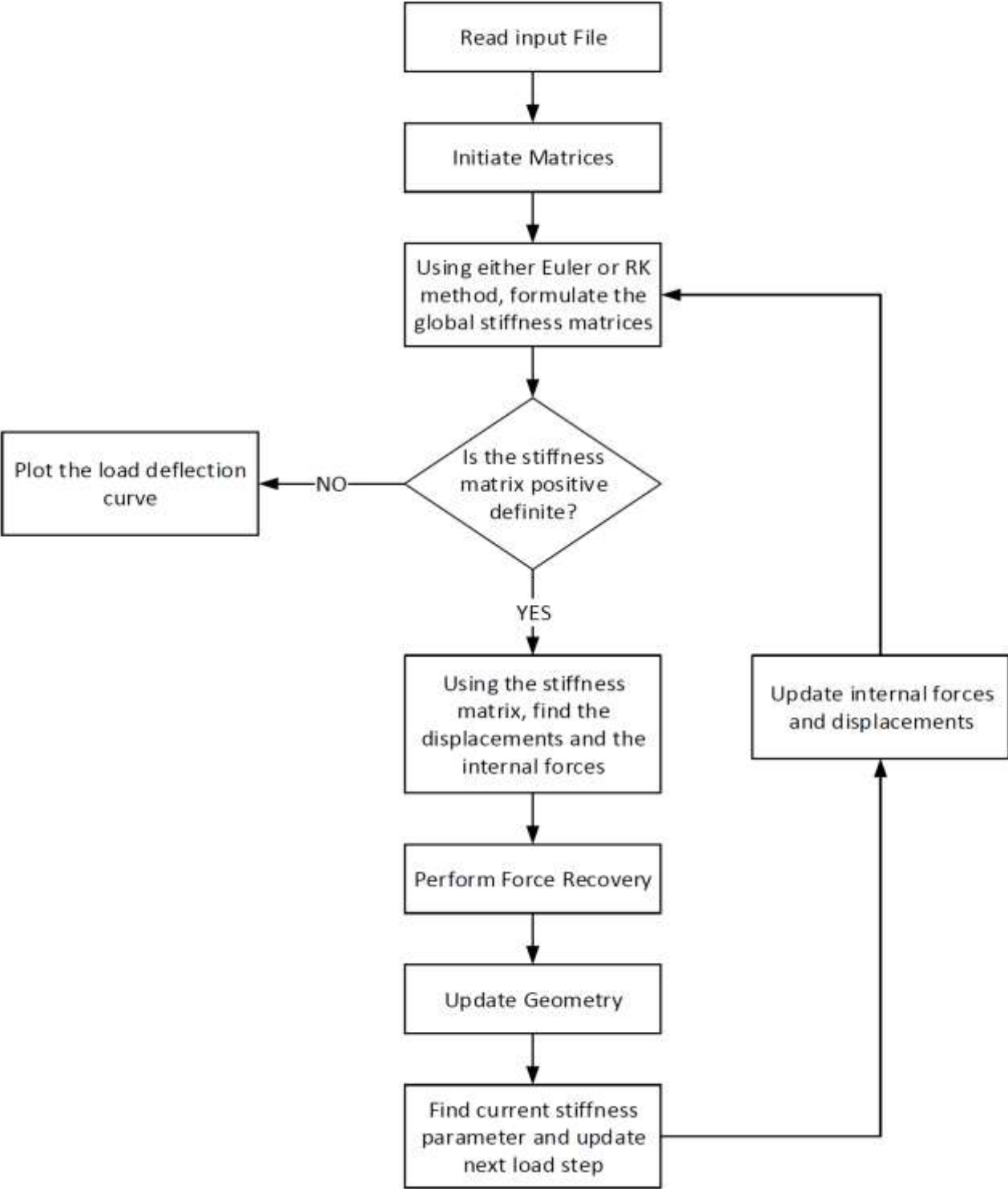
7. Appendix

7.1 Flowchart for Elastic Critical Load Analysis
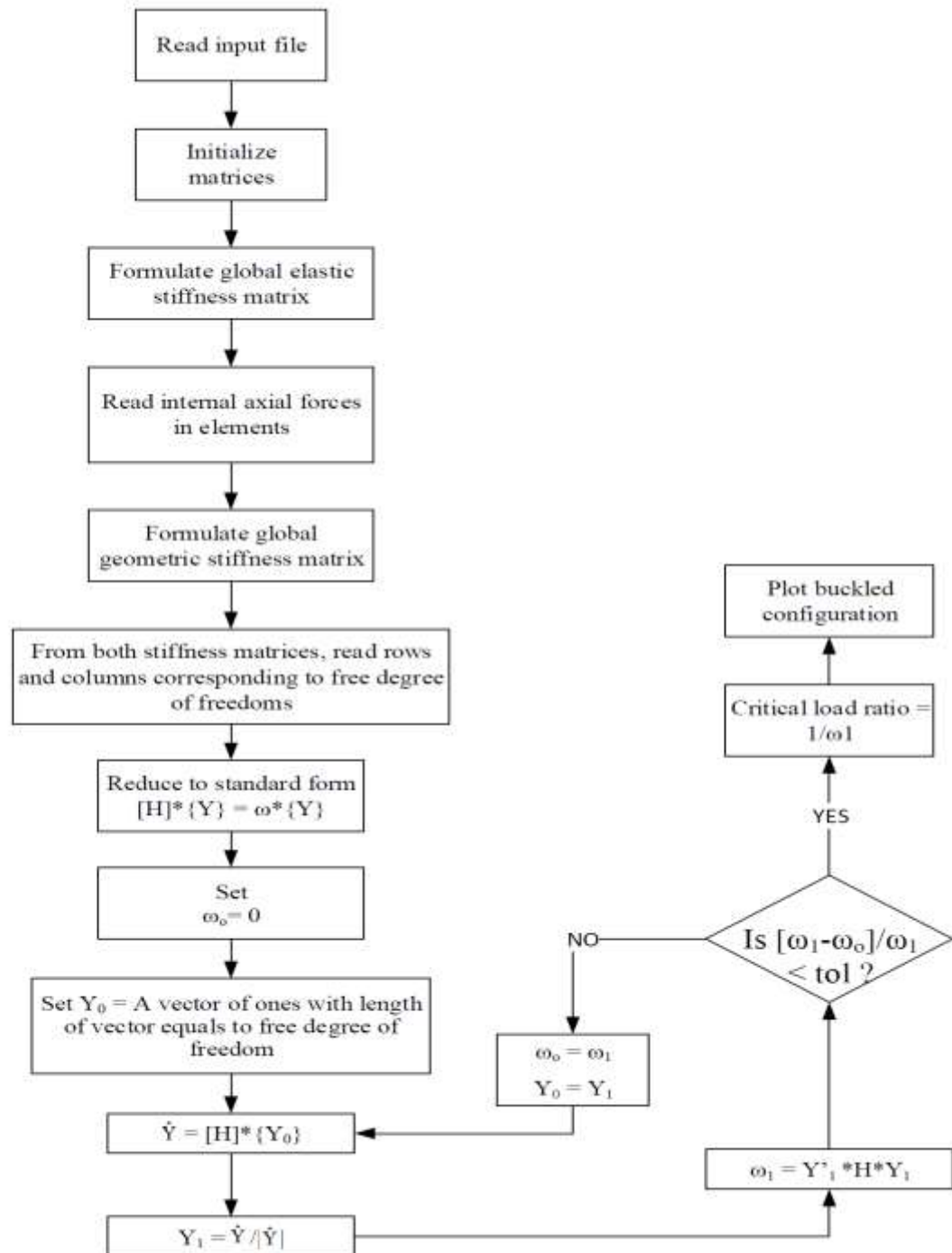
7.2 Flowchart for Inelastic Critical Load Analysis

```
┌─────────────┐    ┌─────────────┐    ┌──────────────────┐    ┌──────────────┐
│Read input   │───▶│ Initialize  │───▶│Run elastic critical│──▶│Find elastic  │
│file         │    │ Matrices    │    │buckling Analysis │    │critical load │
└─────────────┘    └─────────────┘    └──────────────────┘    └──────────────┘
                                                                      │
                                                                      ▼
┌──────────┐         ◇               ┌───────────┐  ┌──────────────────┐  ┌────────────┐
│Elastic   │◀─NO─ Does internal ◀────│Find internal│◀│Run an elastic analysis│◀│Set elastic │
│buckling  │      stress in          │axial stresses│ │based on the referenced│ │critical load│
│controls  │      any element exceed │σ = Fx1 /A  │  │load to find internal  │ │as reference │
└──────────┘      half the yield     └───────────┘  │axial forces           │ │load        │
                  stress?                            └──────────────────┘  └────────────┘
                     │
                    YES
                     ▼
              ┌──────────────────┐     ┌──────────────────┐
              │Inelastic buckling│────▶│      Assume       │
              │occurs            │     │ λmin = 0.001 (a) │
              └──────────────────┘     │ λmax=1 (b)       │
                                       └──────────────────┘
```

$$\lambda_{min} = 0.001 \ (a)$$
$$\lambda_{max}=1 \ (b)$$

Find λ for λ_{max} from eq- 3.10   f(b)

Find λ for λ_{min} from eq- 3.10   f(a)

Find root

$$\models b - \frac{[f(b) - 1](a - b)}{f(a) - f(b)}$$

Find λ setting λ equal to root   f(root)

tol=1-f(root)

Set λ_{max} = root

NO

Does $f(\lambda_{max})$-1 & f(root)-1 have same sign?

Set λ_{min} = root

YES

Is tol < 0.0001

NO

YES

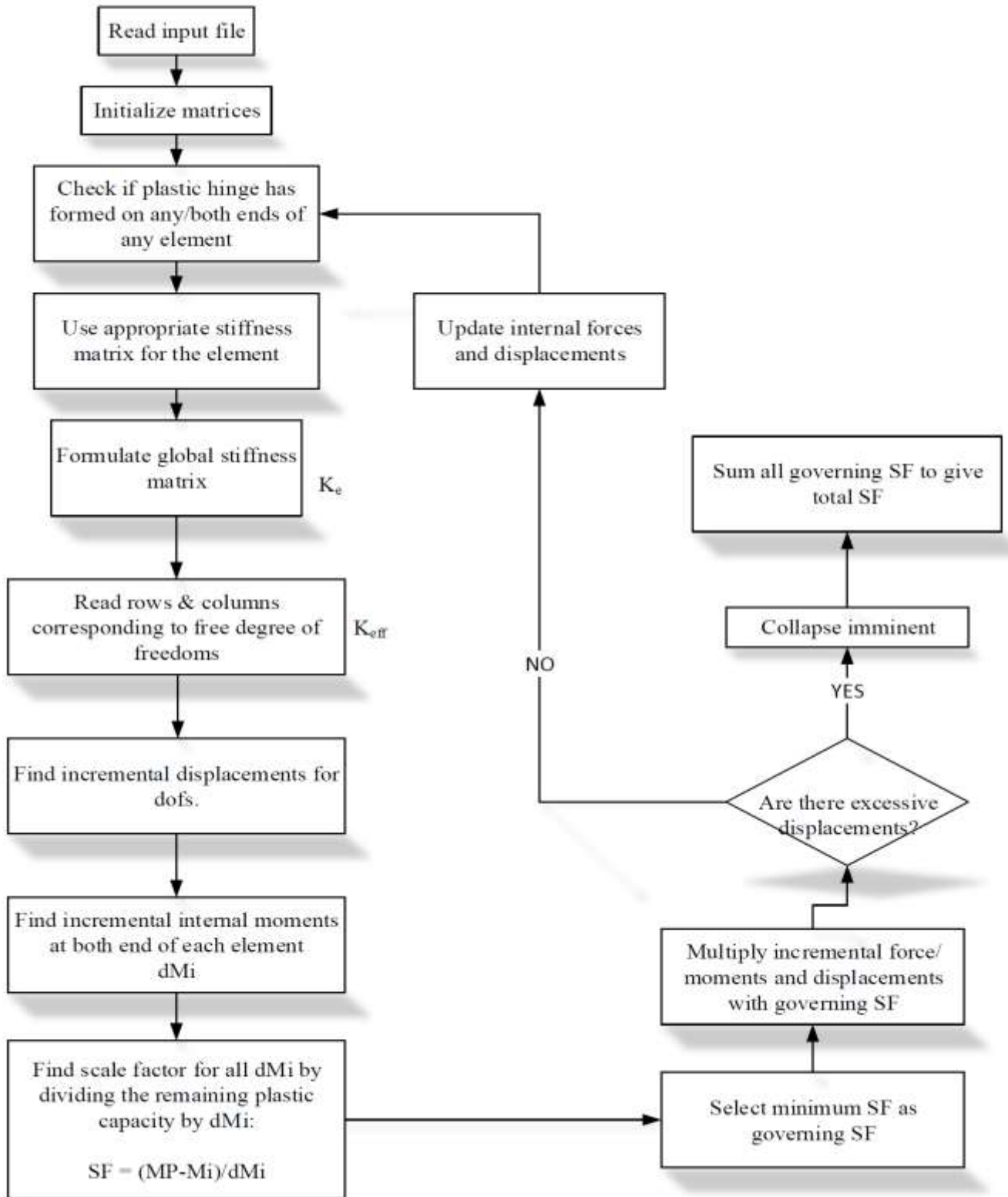Inelastic critical buckling load = root * reference load

Plot buckled configuration

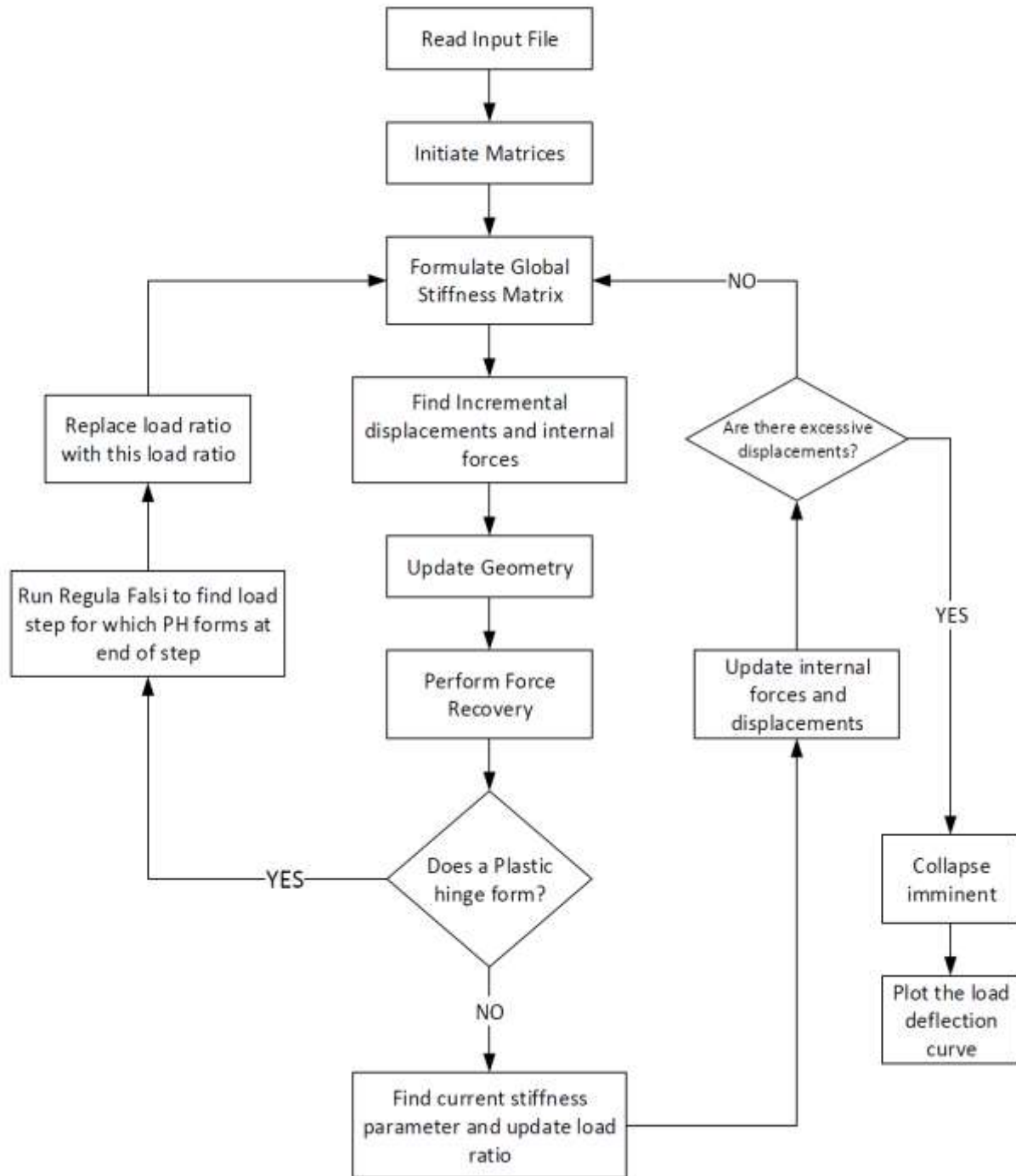## 7.3 Flowchart for Second Order Elastic Analysis

7.4 Flowchart for First Order Inelastic Analysis

7.5 Flowchart for Second Order Inelastic Analysis

7.6 Elemental Stiffness Matrices

7.6.1 Elastic Stiffness Matrix

$$
[K_e] = \begin{bmatrix}
\dfrac{AE}{L} & 0 & 0 & -\dfrac{AE}{L} & 0 & 0 \\[2ex]
0 & \dfrac{12EI}{L^3} & \dfrac{6EI}{L^2} & 0 & -\dfrac{12EI}{L^3} & \dfrac{6EI}{L^2} \\[2ex]
0 & \dfrac{6EI}{L^2} & \dfrac{4EI}{L} & 0 & -\dfrac{6EI}{L^2} & \dfrac{2EI}{L} \\[2ex]
-\dfrac{AE}{L} & 0 & 0 & \dfrac{AE}{L} & 0 & 0 \\[2ex]
0 & -\dfrac{12EI}{L^3} & -\dfrac{6EI}{L^2} & 0 & \dfrac{12EI}{L^3} & -\dfrac{6EI}{L^2} \\[2ex]
0 & \dfrac{6EI}{L^2} & \dfrac{2EI}{L} & 0 & -\dfrac{6EI}{L^2} & -\dfrac{4AE}{L}
\end{bmatrix}
$$

7.6.2 Geometric Stiffness Matrix

$$
[K_g] = \frac{F_{X2}}{L}\begin{bmatrix}
1 & 0 & 0 & -1 & 0 & 0 \\[2ex]
0 & \dfrac{6}{5} & \dfrac{L}{10} & 0 & -\dfrac{6}{5} & \dfrac{L}{10} \\[2ex]
0 & \dfrac{L}{10} & \dfrac{2L^2}{15} & 0 & -\dfrac{L}{10} & -\dfrac{L^2}{30} \\[2ex]
-1 & 0 & 0 & 1 & 0 & 0 \\[2ex]
0 & -\dfrac{6}{5} & -\dfrac{L}{10} & 0 & \dfrac{6}{5} & -\dfrac{L}{10} \\[2ex]
0 & \dfrac{L}{10} & -\dfrac{L^2}{30} & 0 & -\dfrac{L}{10} & \dfrac{2L^2}{15}
\end{bmatrix}
$$